



HAL
open science

Activity-dependent inhibitory synapse scaling is determined by gephyrin phosphorylation and subsequent regulation of GABAA receptor diffusion

Sereina Battaglia, Marianne Renner, Marion Russeau, Etienne Côme, K. Tyagarajan Shiva, Sabine Lévi

► To cite this version:

Sereina Battaglia, Marianne Renner, Marion Russeau, Etienne Côme, K. Tyagarajan Shiva, et al.. Activity-dependent inhibitory synapse scaling is determined by gephyrin phosphorylation and subsequent regulation of GABAA receptor diffusion. *eNeuro*, 2018, 10.1523/ENEURO.0203-17.2017. hal-03977654

HAL Id: hal-03977654

<https://hal.sorbonne-universite.fr/hal-03977654>

Submitted on 7 Feb 2023

HAL is a multi-disciplinary open access archive for the deposit and dissemination of scientific research documents, whether they are published or not. The documents may come from teaching and research institutions in France or abroad, or from public or private research centers.

L'archive ouverte pluridisciplinaire **HAL**, est destinée au dépôt et à la diffusion de documents scientifiques de niveau recherche, publiés ou non, émanant des établissements d'enseignement et de recherche français ou étrangers, des laboratoires publics ou privés.

1 **1. Title:** Activity-dependent inhibitory synapse scaling is determined by gephyrin
2 phosphorylation and subsequent regulation of GABA_A receptor diffusion.

3
4
5 **2. Abbreviated Title:** Gephyrin phosphorylation shapes GABA_AR diffusion

6
7 **3. Authors and affiliations :**

8 Sereina Battaglia⁴, Marianne Renner^{1,2,3}, Marion Rousseau^{1,2,3}, Etienne Côme^{1,2,3}, Shiva
9 K. Tyagarajan^{4,5¥}, Sabine Lévi^{1,2,3¥}

10
11 ¹ INSERM UMR-S 839, 75005, Paris, France

12 ² Université Pierre et Marie Curie, 75005, Paris, France

13 ³ Institut du Fer a Moulin, 75005, Paris, France;

14 ⁴ Institute of Pharmacology and Toxicology, University of Zürich, 8057 Zurich, CH

15 ⁵ Center for Neuroscience Zurich, Winterthurerstrasse 190, 8057 Zurich, CH

16
17 ¥ co-senior authors

18
19 **4. Author contributions:**

20 SL and SKT conceptualized the project and designed the experiments. SL supervised
21 the experimental work. SB, EC and M. Ru performed immunofluorescence and SPT
22 experiments and analyzed the data together with SL. M. Ru prepared primary
23 hippocampal neurons. MRe performed the super-resolution experiments, developed
24 data analysis tools and analyzed the data. SL and SKT wrote the manuscript.

25
26 **5. Correspondence should be addressed to:**

27 Sabine Lévi

28 INSERM-UPMC UMR-S 839

29 17 rue du Fer a Moulin

30 75005 Paris, France

31 Tel. +33 1 45 87 61 13

32 E-mail: sabine.levi@inserm.fr

33
34 Shiva Tyagarajan

35 Institute of Pharmacology and Toxicology

36 University of Zürich

37 Winterthurerstrasse 190, 8057 Zurich, CH

38 Tel: +41 44 6355997

39 E-mail: tyagarajan@pharma.uzh.ch

40
41 **6. Number of Figures :** 8

42 **7. Number of Tables :** 0

43 **8. Number of Multimedia :** 0

44 **9. Number of words for Abstract:** 128

45 **10. Number of words for Significance Statement:** 36

46 **11. Number of words for Introduction:** 461

47 **12. Number of words for Discussion:** 1204

48

49

50

1 **13. Acknowledgements:**

2 We are grateful to the Cell and Tissue Imaging Facility of Institut du Fer à Moulin
3 (IFM). This work was supported in part by INSERM, Sorbonne Université-UPMC,
4 LabEx Biopsy to SL, Olgamyenfisch Grant to SKT and University of Zurich internal
5 funding to SKT. EC is the recipient of a doctoral fellowship from the Université Pierre
6 and Marie Curie. STORM/PALM equipment at the IFM was supported by DIM NeRF
7 from Région Ile-de-France and by the FRC/Rotary 'Espoir en tête'. The Lévi lab is
8 affiliated with the Paris School of Neuroscience (ENP) and the Bio-Psy Laboratory of
9 excellence.

10

11 **14. Conflict of interest:**

12 No. The authors report no conflict of interest in relation to the submitted work.

13

14 **15. Funding sources:**

15 This work was supported in part by INSERM, Sorbonne Université-UPMC, LabEx
16 Biopsy to SL, Olgamyenfisch Grant to SKT and University of Zurich internal funding
17 to SKT. EC is the recipient of a doctoral fellowship from the Université Pierre and
18 Marie Curie. STORM/PALM equipment at the IFM was supported by DIM NeRF from
19 Région Ile-de-France and by the FRC/Rotary 'Espoir en tête'. The Lévi lab is affiliated
20 with the Paris School of Neuroscience (ENP) and the Bio-Psy Laboratory of excellence.

21

22

1 **Activity-dependent inhibitory synapse scaling is determined by gephyrin**
2 **phosphorylation and subsequent regulation of GABA_A receptor diffusion.**

3
4
5
6 **Abstract:**

7 Synaptic plasticity relies on the rapid changes in neurotransmitter receptor number at
8 postsynaptic sites. Using super resolution PALM imaging and quantum-dot based
9 single particle tracking in rat hippocampal cultured neurons, we investigated if the
10 phosphorylation status of the main scaffolding protein gephyrin influenced the
11 organization of the gephyrin scaffold and GABA_A receptor (GABA_AR) membrane
12 dynamics. We found that gephyrin phosphorylation regulates gephyrin microdomain
13 compaction. The ERK1/2 and GSK3 β signaling alter the gephyrin scaffold mesh
14 differentially. Differences in scaffold organization impacted similarly the diffusion of
15 synaptic GABA_ARs, suggesting reduced gephyrin-receptor binding properties. In the
16 context of synaptic scaling, our results identify a novel role of the GSK3 β signaling
17 pathway in the activity-dependent regulation of extrasynaptic receptor surface
18 trafficking and GSK3 β , PKA and CaMKII α pathways in facilitating adaptations of
19 synaptic receptors.

20
21

22 **Significance Statement:**

23 Our data identify phosphorylation as a key mechanism controlling the gephyrin scaffold
24 mesh, and hence, the diffusion capture of GABA_A receptors at inhibitory synapses. We
25 further show how critical this mechanism is for inhibitory synaptic scaling.

26

1 **Introduction:**

2 Fast synaptic inhibition mediated by GABA_ARs plays an essential role in information
3 transfer between neurons. In recent years GABAergic inhibition has been shown to be
4 dynamic, allowing flexible adaptations (Chen et al., 2012). Within the paradigm of in-
5 vitro synaptic scaling, wherein the neuronal activity is pharmacologically manipulated
6 for several hours to days, the effects of chronic changes in activity are still poorly
7 understood at inhibitory synapses.

8 Neuronal inhibition is dynamically regulated by the amount of network activity.
9 GABA_AR stability at synaptic sites and subsequent proteasomal degradation is an
10 essential component of synaptic homeostasis that strongly influences amplitude and
11 frequency of miniature inhibitory postsynaptic currents (mIPSCs) (Saliba et al., 2007).

12 Similarly, lasting depolarization decreases GABA_AR internalization on principal
13 neurons and increases GAD65 cluster size at presynaptic GABAergic terminals
14 (Rannals and Kapur, 2011). These observations highlight that multiple systems and
15 pathways facilitate inhibitory synapse adjustments in response to chronic changes in
16 activity.

17 At postsynaptic sites lateral diffusion in and out of synapses can also rapidly alter
18 receptor availability upon acute activity elevation (Bannai et al., 2009; 2015). Chemical
19 induced long-term potentiation (iLTP) enhances phosphorylation of the GABA_AR β 3
20 subunit at S383 by CaMKII α , resulting in reduced surface mobility of GABA_ARs,
21 synaptic enrichment of receptors and increased inhibitory neurotransmission (Petrini et
22 al., 2014). Hence, apart from endocytosis and exocytosis, lateral diffusion of receptors
23 could also be an effective mechanism of synaptic plasticity.

24 In recent years it has become evident that the main scaffolding protein at the
25 GABAergic synapse, gephyrin, is dynamically regulated, and this contributes to input-

1 specific adaptations at postsynaptic sites (Chen et al., 2012; van Versendaal et al., 2012;
2 Villa et al., 2016). Identification of signaling pathways that converge onto gephyrin
3 scaffolds by causing post-translational modifications of specific residues has shed new
4 light into the molecular mechanisms underlying GABAergic synaptic plasticity. It was
5 revealed that gephyrin phosphorylation by ERK1/2 at serine 268 (S268) reduces
6 scaffold size and GABAergic mIPSC amplitude (Tyagarajan et al., 2013). Similarly,
7 blocking GSK3 β phosphorylation of gephyrin at serine 270 via the transgenic
8 expression of the phospho-null mutant (S270A) significantly increases mIPSC
9 frequency and amplitude (Tyagarajan et al., 2011). Theta burst stimulation (TBS) of
10 CA3 Schaffer collaterals has been reported to induce gephyrin-mediated remodeling of
11 GABAergic synapses in CA1 pyramidal cells (Flores et al., 2015). Although gephyrin
12 phosphorylation at CaMKII α sites is involved in this form of structural plasticity
13 (Flores et al., 2015), the molecular basis for gephyrin phosphorylation induced
14 GABA_AR synapse dynamics remains to be further explored.

15 To address this we rendered gephyrin insensitive to ERK1/2 and GSK3 β signaling
16 pathways and studied their influence on GABA_AR membrane diffusion properties. We
17 report structural organization differences within gephyrin scaffolds based on their
18 phosphorylation status. Furthermore, cooperation between gephyrin and GABA_ARs are
19 differentially regulated by gephyrin phosphorylation status and changes in activity.

20

21

22

23

24

25

1 **Material and Methods**

2 *Neuronal culture*

3 Primary cultures of hippocampal neurons were prepared from hippocampi dissected at
4 embryonic day 18 or 19 from Sprague-Dawley rats of either sex. Tissue was then
5 trypsinized (0.25% v/v), and mechanically dissociated in 1x HBSS (Invitrogen, Cergy
6 Pontoise, France) containing 10 mM HEPES (Invitrogen). Neurons were plated at a
7 density of 120×10^3 cells/ml onto 18-mm diameter glass coverslips (Assistent,
8 Winigor, Germany) pre-coated with 50 μ g/ml poly-D,L-ornithine (Sigma-Aldrich,
9 Lyon, France) in plating medium composed of Minimum Essential Medium (MEM,
10 Sigma) supplemented with horse serum (10% v/v, Invitrogen), L-glutamine (2 mM)
11 and Na⁺ pyruvate (1 mM) (Invitrogen). After attachment for 3-4 h, cells were incubated
12 in culture medium that consists of Neurobasal medium supplemented with B27 (1X),
13 L-glutamine (2 mM), and antibiotics (penicillin 200 units/ml, streptomycin, 200 μ g/ml)
14 (Invitrogen) for up to 4 weeks at 37°C in a 5% CO₂ humidified incubator. Each week,
15 one fifth of the culture medium volume was replaced.

16

17 *DNA constructs*

18 The following constructs were used: *GEPHN* 3'-UTR shRNA and control shRNA-3m
19 (Yu et al., 2007), DsRed-homer1c (Bats et al., 2007) (kindly provided by D. Choquet,
20 IIN, Bordeaux, France), eGFP-gephyrin P1 variant (Lardi-Studler et al., 2007), and
21 eGFP- or pDendra2- WT, -S268E, S270A, -DN, -S303A/S305A (SSA) and –
22 SSA/S270A point mutants were generated using the eGFP-gephyrin P1 variant as
23 template for site directed mutagenesis (Tyagarajan et al., 2011; 2013; Flores et al.,
24 2015).

25

1 *Neuronal transfection*

2 Transfections were carried out at DIV 14-15 using Lipofectamine 2000 (Invitrogen) or
3 Transfectin (BioRad, Hercules, USA), according to the manufacturers' instructions
4 (DNA:transfectin ratio 1 µg:3 µl), with 1-1.2 µg of plasmid DNA per 20 mm well. The
5 following ratios of plasmid DNA were used in co-transfection experiments: 0.5:0.5:0.3
6 µg for eGFP-S268E/eGFP-S270A/eGFP-DN/eGFP-SSA/eGFP-SSA/S270A: *GEPHN*
7 3' UTR shRNA/*GEPHN* 3' UTR-3m shRNA: DsRed-homer1c. Experiments were
8 performed 6 to 9 days post-transfection.

9

10 *Pharmacology*

11 4-aminopyridine (4-AP, 100 mM, Sigma) was directly added to the culture medium and
12 the neurons were returned to a 5% CO₂ humidified incubator for 8 or 48 h before use.
13 For SPT experiments, neurons were labeled at 37°C in imaging medium (see below for
14 composition) in presence of 4-AP, transferred to a recording chamber and recorded
15 within 45 min at 31°C in imaging medium in the presence of 4-AP. The imaging
16 medium consisted of phenol red-free minimal essential medium supplemented with
17 glucose (33 mM; Sigma) and HEPES (20 mM), glutamine (2 mM), Na⁺-pyruvate (1
18 mM), and B27 (1X) from Invitrogen.

19

20 *Immunocytochemistry*

21 Cells were fixed for 15 min at room temperature (RT) in paraformaldehyde (PFA, 4%
22 w/v, Sigma) and sucrose (14% w/v, Sigma) solution prepared in PBS (1X). Following
23 washes in PBS, cells were permeabilized with Triton (0.25% v/v, Sigma) diluted in
24 PBS. Cells were washed again in PBS and incubated for 1 h at RT in Triton (0.1% v/v,
25 Sigma) and goat serum (GS, 10% v/v, Invitrogen) in PBS to block nonspecific staining.

1 Subsequently, neurons were incubated for 1 h with a primary antibody mix consisting
2 of guinea pig antibodies against GABA_AR α 2 subunit (1:2000, provided by J.M.
3 Fritschy, Univ. Zurich) and rabbit anti-VGAT (1:400, provided by B. Gasnier, Univ.
4 Paris Descartes, Paris) in PBS supplemented with GS (10% v/v, Invitrogen) and Triton
5 (0.1%v/v, Sigma). After washes, cells were incubated for 60 min at RT with a
6 secondary antibody mix containing biotinylated F(ab')₂ anti-guinea pig (1:300, Jackson
7 Immunoresearch) and AMCA350-conjugated goat anti rabbit (1:100, Jackson
8 Laboratories) in PBS-GS-Triton blocking solution, washed, incubated for another 45
9 min with streptavidin-CY5 (1:300, ThermoFisher) and finally mounted on glass slides
10 using Mowiol 4-88 (48 mg/ml, Sigma). Sets of neurons compared for quantification
11 were labeled simultaneously.

12

13 *Fluorescence image acquisition and analysis*

14 Image acquisition was performed using a 63 X objective (NA 1.32) on a Leica
15 (Nussloch, Germany) DM6000 upright epifluorescence microscope with a 12-bit
16 cooled CCD camera (Micromax, Roper Scientific) run by MetaMorph software (Roper
17 Scientific, Evry, France). Quantification was performed using MetaMorph software
18 (Roper Scientific). Image exposure time was determined on bright cells to obtain best
19 fluorescence to noise ratio and to avoid pixel saturation. All images from a given culture
20 were then acquired with the same exposure time and acquisition parameters. For each
21 image, several dendritic regions of interest were manually chosen and a user-defined
22 intensity threshold was applied to select clusters and avoid their coalescence. For
23 quantification of gephyrin or GABA_AR α 2 synaptic clusters, gephyrin or receptor
24 clusters comprising at least 3 pixels and colocalized on at least 1 pixel with VGAT

1 clusters were considered. The integrated fluorescence intensities of clusters were
2 measured.

3

4 *Live cell staining for single particle imaging*

5 Neurons were incubated for 3-5 min at 37°C with primary antibodies against
6 extracellular epitopes of GABA_AR α2 subunit (guinea pig, 1:750/1:1000 provided by
7 J.M. Fritschy), washed, and incubated for 3-5 min at 37°C with biotinylated Fab
8 secondary antibodies (goat anti-guinea pig, 4-12µg/ml; Jackson Immuno research,
9 West Grove, USA) in imaging medium. After washes, cells were incubated for 1 min
10 with streptavidin-coated quantum dots (QDs) emitting at 605 nm (1 nM; Invitrogen) in
11 borate buffer (50 mM) supplemented with sucrose (200 mM) or in PBS (1M;
12 Invitrogen) supplemented with 10% Casein (v/v) (Sigma). Washing and incubation
13 steps were all done in imaging medium. To assess the membrane dynamics of GABA_AR
14 α2 subunit at inhibitory synapses in neurons expressing the eGFP-DN mutant,
15 inhibitory synapses were stained by incubating live neurons for 48 h at 37°C in a 5%
16 CO₂ humidified incubator with a primary VGAT antibody directly coupled to
17 Oyster550 (1:200, Synaptic Systems) diluted in conditioned maintenance medium.

18

19 *Single particle tracking and analysis*

20 Cells were imaged using an Olympus IX71 inverted microscope equipped with a 60X
21 objective (NA 1.42; Olympus) and a Lambda DG-4 monochromator (Sutter
22 Instrument). Individual images of gephyrin-eGFP and homer1c-GFP, and QD real time
23 recordings (integration time of 75 ms over 600 consecutive frames) were acquired with
24 Hamamatsu ImagEM EMCCD camera and MetaView software (Meta Imaging 7.7).
25 Cells were imaged within 45 min following labeling.

1 QD tracking and trajectory reconstruction were performed with Matlab software (The
2 Mathworks, Natick, MA). One to two sub-regions of dendrites were quantified per cell.
3 In cases of QD crossing, the trajectories were discarded from analysis. Trajectories
4 were considered synaptic when overlapping with the synaptic mask of gephyrin-eGFP
5 or VGAT-Oyster550 clusters, or extrasynaptic for spots two pixels (380 nm) away
6 (Lévi et al., 2008). Values of the mean square displacement (MSD) plot versus time
7 were calculated for each trajectory by applying the relation:

$$8 \quad MSD(n\tau) = \frac{1}{N-n} \sum_{i=1}^{N-n} \left[(x((i+n)\tau) - x(i\tau))^2 + (y((i+n)\tau) - y(i\tau))^2 \right]$$

9 (Saxton and Jacobson, 1997), where τ is the acquisition time, N is the total number of
10 frames, n and i are positive integers with n determining the time increment. Diffusion
11 coefficients (D) were calculated by fitting the first four points without origin of the
12 MSD versus time curves with the equation: $MSD(n\tau) = 4Dn\tau + b$ where b is a constant
13 reflecting the spot localization accuracy. Synaptic dwell time was defined as the
14 duration of detection of QDs at synapses on a recording divided by the number of exits
15 as detailed previously (Ehrensperger et al., 2007; Charrier et al., 2010). Dwell times ≤ 5
16 frames were not retained. The explored area of each trajectory was defined as the MSD
17 value of the trajectory at two different time intervals of at 0.42 and 0.45 s (Renner et
18 al., 2012).

19

20 *PALM imaging*

21 PALM imaging on fixed samples was carried out on an inverted N-STORM Nikon
22 Eclipse Ti microscope with a 100x oil-immersion objective (N.A. 1.49) and an Andor
23 iXon Ultra EMCCD camera (image pixel size, 160 nm), using specific lasers for PALM
24 imaging of Dendra2 (405 and 561 nm). Movies of 10000 frames were acquired at frame

1 rates of 50 ms. The z position was maintained during acquisition by a Nikon perfect
2 focus system. Single-molecule localization and 2D image reconstruction was
3 conducted as described in (Specht et al., 2013) by fitting the PSF of spatially separated
4 fluorophores to a 2D Gaussian distribution. The position of fluorophore were corrected
5 by the relative movement of the synaptic cluster by calculating the center of mass of
6 the cluster throughout the acquisition using a partial reconstruction of 2000 frames with
7 a sliding window (Specht et al., 2013). PALM images were rendered by superimposing
8 the coordinates of single-molecule detections, which were represented with 2D
9 Gaussian curves of unitary intensity and SDs representing the localization accuracy
10 ($\sigma = 20$ nm). In order to correct multiple detections coming from the same
11 pDendra2 molecule (Specht et al., 2013), we identified detections occurring in the
12 vicinity of space ($2 \times \sigma$) and time (15 s) as belonging to a same molecule. The
13 surface of gephyrin clusters and the densities of gephyrin molecules per μm^2 were
14 measured in reconstructed 2D images through cluster segmentation based on detection
15 densities. The threshold to define the border was set to 1000 detections/ μm^2 , taking into
16 account the reported gephyrin densities in synapses (Specht et al, 2013; Fig. 3B).
17 Briefly, all pixels (PALM pixel size=20 nm) containing less than 2 detections were
18 considered as empty, and their intensity value set to zero. The intensity of pixels with
19 at least two detections was set to one. The resulting binary image was analyzed with
20 the function regionprops of Matlab (The Mathworks) to extract the surface area of each
21 cluster identified by this function. Density was calculated as the total number of
22 detections in the pixels belonging to a given cluster, divided the area of the cluster.

23

24

25

1 *Statistics*

2 Sampling corresponds to the number of quantum dots for SPT, the number of cells for
3 ICC, and the number of synapses for PALM. Sample size selection for experiments was
4 based on published experiments, pilot studies as well as in-house expertise. All results
5 were used for analysis except in few cases. Cells with signs of suffering (apparition of
6 blobs, fragmented neurites) were discarded from the analysis. Means are shown \pm SEM,
7 median values are indicated with their interquartile range (IQR, 25-75%). Means were
8 compared using the non-parametric Mann-Whitney test (immunocytochemistry, dwell
9 time comparison, PALM quantifications) using SigmaPlot 12.5 software (Systat
10 Software). Diffusion coefficient and explored area values having non-normal
11 distributions, a non-parametric Kolmogorov-Smirnov test was run under Matlab (The
12 Mathworks, Natick, MA). Differences were considered significant for p-values less
13 than 5% ($*p \leq 0.05$; $**p < 0.01$; $***p < 0.001$).

14
15

16 **Results:**

17 **eGFP-gephyrin mutants exhibit different clustering properties in culture.**

18 Signaling pathways that converge onto gephyrin scaffolding properties influence
19 GABA_AR synaptic transmission. Hence, mimicking phosphorylation/
20 dephosphorylation events that influence gephyrin clustering can help gain critical
21 insights into nanoscale regulation of GABA_ARs at synaptic sites. ERK1/2
22 phosphorylation at the S268 residue results in smaller gephyrin clusters (Tyagarajan et
23 al., 2013); hence, we selected phospho-mimetic eGFP-gephyrin-S268E mutant to study
24 the impact of smaller clusters on receptor diffusion. Similarly, pharmacological
25 blockade of the GSK3 β pathway or eGFP-gephyrin-S270A mutant expression

1 increases gephyrin cluster number and size (Tyagarajan et al., 2011). We selected the
2 eGFP-S270A mutant to understand how larger clusters would impact receptor
3 diffusion. eGFP-gephyrin dominant negative (DN) mutant in primary neurons not only
4 abolishes gephyrin clustering, reduces surface expression of GABA_ARs, but also
5 significantly decreases GABAergic mIPSC amplitude and frequency (Ghosh et al.,
6 2016). Hence, we selected eGFP-DN mutant to evaluate how cluster disruption would
7 impact synaptic anchoring and surface diffusion of GABA_ARs.

8 Primary hippocampal neurons were co-transfected at 14 days *in vitro* (DIV) with eGFP-
9 gephyrin WT (eGFP-WT), eGFP-S268E, eGFP-S270A or eGFP-DN along with
10 shRNA targeting the gephyrin 3'UTR (to minimize the influence of endogenous
11 gephyrin expression on mutant phenotypes). Before studying the influence of altered
12 gephyrin clustering on GABA_AR diffusion properties we first confirmed the respective
13 gephyrin mutant morphology 6-9 days post-transfection. Representative images of
14 neurons expressing either eGFP-WT or eGFP-S268E, eGFP-S270A, eGFP-DN
15 variants are shown (Fig. 1A). We stained for the $\alpha 2$ GABA_AR subunit to study the
16 relation of eGFP-gephyrin with receptors. Quantification for eGFP-gephyrin cluster
17 density (Nb), cluster size (area) and intensity (Int) showed a tendency for reduced
18 clustering for the S268E mutant, and increased clustering for the S270A mutant (Fig
19 1B). The impact of the gephyrin S270A mutation on gephyrin cluster area and intensity
20 was more pronounced, in comparison to S268E mutant. As expected eGFP-DN failed
21 to cluster (data not shown). Similar to the observed changes in eGFP-gephyrin
22 morphology, quantification of cluster intensity for $\alpha 2$ GABA_AR showed a significant
23 increase in neurons expressing eGFP-S270A, while eGFP-S268E expressing neurons
24 only showed a modest reduction in $\alpha 2$ (Fig. 1C). The neurons expressing eGFP-DN
25 showed very little $\alpha 2$ GABA_AR staining (data not shown).

1

2 **Influence of eGFP-gephyrin mutants on GABA_AR surface diffusion.**

3 GABA_ARs are known to exhibit faster mobility at extrasynaptic sites as compared with
4 synaptic sites. Due to their interaction with the main scaffolding molecule gephyrin
5 GABA_ARs are slowed down and confined at synapses. This diffusion-capture of
6 GABA_ARs is modulated by neuronal activity and constitutes an important basis for
7 synaptic plasticity (ref in (Petrini and Barberis, 2014)). The expression of specific
8 eGFP-gephyrin mutation allows us to lock the scaffold into different conformations and
9 study its influence on GABA_AR surface diffusion. To achieve this we assessed the
10 lateral mobility of $\alpha 2$ GABA_AR using quantum-dot (QD) based single particle tracking
11 (QD-SPT). Live imaging over 600 constitutive frames at 75 Hz was used to record
12 individual trajectories, and the trajectories were later analyzed using custom software
13 (Fig. 2A) (see Material and Methods). As a proof of concept we first tested the effect
14 of total gephyrin cluster removal on $\alpha 2$ GABA_AR surface dynamics by expressing the
15 eGFP-DN mutant. However, given that eGFP-DN has a diffuse expression, to
16 distinguish synaptic and extra-synaptic $\alpha 2$ clusters we pre-loaded presynaptic
17 GABAergic terminals using VGAT-Oyster550 antibody. The expression of the eGFP-
18 DN mutant increased the surface exploration of QDs at both extrasynaptic and synaptic
19 sites compared with control eGFP-WT. Quantification of the $\alpha 2$ GABA_AR diffusion
20 coefficient showed a 1.4 fold increase for extrasynaptic receptors and 1.2 fold increase
21 for synaptic receptors in eGFP-DN expressing neurons (Fig. 2B). Area explored by $\alpha 2$
22 GABA_ARs also showed a 1.6 fold increase at extrasynaptic sites and a 1.3 fold increase
23 at synaptic sites in eGFP-DN expressing neurons (Fig. 2C). These observations support
24 the notion that gephyrin not only slows down and confines GABA_ARs at synapses but
25 also at extrasynaptic sites (Ehrensperger et al., 2007).

1 Synaptic dwell time values can be discriminated from “trapped” receptors (dwell
2 time > 5.9 s) and “passing” receptors (dwell time ≤ 5.9 s) (Renner et al., 2012).
3 Quantification of $\alpha 2$ GABA_AR dwell time confirmed a 1.3 fold faster escape time of
4 receptors in neurons expressing the eGFP-DN mutant (Fig. 2D). We did not observe
5 any difference in this rate for passing receptors. This is an indication that the observed
6 reduction of trapped receptors is not due to increased membrane viscosity, but rather
7 due to gephyrin scaffold’s influence on GABA_AR surface mobility. Thus, we concluded
8 that the diffuse DN gephyrin relieved GABA_AR $\alpha 2$ diffusion constraints leading to
9 synaptic escape of receptors.

10 If indeed gephyrin clustering can influence receptor diffusion, then S268E and S270A
11 modification(s) must have an influence on $\alpha 2$ GABA_AR surface mobility. To test this,
12 we transfected the eGFP-S268E or eGFP-S270A mutants and measured surface
13 mobility at extrasynaptic and synaptic locations. Superimposition of trajectories with
14 fluorescent image of eGFP-gephyrin allowed us to distinguish synaptic versus
15 extrasynaptic $\alpha 2$ GABA_ARs. Neurons transfected with eGFP-S268E exhibited an
16 increase in surface exploration of individual trajectories (Fig. 2A). This was consistent
17 with the observed increase in diffusion coefficients at both extrasynaptic and synaptic
18 sites (Fig. 2E). Similarly, quantification of explored area at both extrasynaptic and
19 synaptic sites showed significant increases (Fig. 2F). If reducing gephyrin cluster size
20 facilitates $\alpha 2$ diffusion, then we expect shorter dwell time at synaptic sites. Indeed, we
21 report reduced dwell time for trapped $\alpha 2$ GABA_ARs in eGFP-S268E transfected
22 neurons (Fig. 2G). Therefore the use of eGFP-S268E gephyrin mutant shows that the
23 reduction in gephyrin cluster size causes increase in GABA_AR diffusion, while
24 reducing synaptic dwell time.

1 On the other hand, in eGFP-S270A transfected neurons, the $\alpha 2$ GABA_ARs showed
2 increased surface exploration of individual trajectories at synapses (Fig. 2A).
3 Unexpectedly, diffusion coefficients and surface exploration of $\alpha 2$ extrasynaptic and
4 synaptic GABA_ARs were significantly increased in eGFP-S270A transfected neurons
5 (Fig. 2E-F). However, analysis showed no reduction in $\alpha 2$ GABA_AR dwell time at
6 synaptic sites (Fig. 2G). We thus concluded that the increase in receptor mobility at
7 synapses in S270A transfected neurons does not correlate with what we may expect
8 from a larger scaffold, suggesting additional regulations are at play.

9

10 **Super-resolution PALM microscopy reveals differential packing of gephyrin** 11 **scaffold.**

12 We turned to quantitative nanoscopic imaging to understand the influence of
13 phosphorylation on gephyrin scaffold organization. Using photoactivated localization
14 microscopy (PALM) we estimated localization accuracy from several detections of the
15 same fluorophore from subsequent image frames (Specht et al., 2013). The spatial
16 resolution of PALM is within the range of ~25-30 nm; hence, image segmentation of
17 the rendered PALM images can resolve substructure organization within a gephyrin
18 cluster, that are not discernable using diffraction limited imaging (Specht et al., 2013).
19 Employing fluorescence imaging on primary hippocampal neurons co-transfected with
20 photo-convertible pDendra2-WT, pDendra2-S268E or pDendra2-S270A and shRNA
21 3'UTR showed a clustering phenotype consistent with eGFP-gephyrin and its mutant
22 variants (Fig. 3A). PALM image cluster segmentation was established based on local
23 density of detections using a threshold of 1000 detections/ μm^2 (Fig. 3B). Image
24 segmentation allows us to estimate the mean surface area of a given pDendra2-WT
25 cluster. In this case quantification showed pDendra2-WT clusters to be $0.054 \pm$

1 0.003 μm^2 , corresponding to the mean diameter of 262 nm as has been reported earlier
2 (Specht et al., 2013). pDendra2-S268E quantifications showed a significant reduction
3 in mean surface area to $0.035 \pm 0.002 \mu\text{m}^2$, and consistent with our expectations,
4 pDendra2-S270A showed an increase in cluster area of $0.078 \pm 0.005 \mu\text{m}^2$ as expected
5 (Fig. 3C).

6 We next tried to correlate the estimated size of gephyrin clusters to their respective
7 densities. Our analysis showed 3919.7 ± 227.9 molecules/ μm^2 of pDendra2-WT
8 molecules within a cluster (Fig. 3D). pDendra2-S268E showed a significantly increased
9 molecular density (4457.5 ± 221.6) in spite of having a smaller cluster area. In contrast,
10 pDendra2-S270A mutant shows a significantly reduced molecular density ($2819.8 \pm$
11 117.6), in spite of having a larger surface area (Fig. 3D).

12 Our data indicate that there is no correlation between the diffusion properties of
13 GABA_ARs in spite of the relative size difference between S268E and S270A gephyrin
14 clusters. However, there is a strong correlation between gephyrin phosphorylation and
15 cluster microdomain compaction. The compaction of the scaffold or the increased
16 spacing between gephyrin molecules may perturb the organization of the gephyrin
17 microdomain thereby altering gephyrin-receptor binding properties. We cannot exclude
18 the possibility that the mutations impact directly receptor-binding properties
19 independently of their effect on the mesh.

20

21 **Prolonged neuronal activity influences gephyrin and GABA_AR clustering as well**
22 **as GABA_AR diffusion.**

23 Activity-dependent regulation of receptor lateral diffusion is an essential contributor to
24 synapse adaptation (Lüscher et al., 2011). This phenomenon has been explored within
25 the experimental paradigm of short-term (1-60 min) drug applications (Bannai et al.,

1 2009; Muir et al., 2010; Niwa et al., 2012; Petrini et al., 2014; Bannai et al., 2015).
2 There is accumulating evidence that synaptic adaptations at GABAergic synapses also
3 occur in response to prolonged changes in activity (Rannals and Kapur, 2011; Vlachos
4 et al., 2013; Flores et al., 2015). Hence, we examined whether gephyrin
5 phosphorylation regulates activity-dependent membrane diffusion and synaptic
6 recruitment of $\alpha 2$ GABA_ARs. To test this hypothesis, we chronically elevated synaptic
7 activity by treating our primary hippocampal neurons with the potassium channel
8 blocker 4-aminopyridine (4-AP; 100 μ M) (Chamma et al., 2013) for 8 h or 48 h. We
9 used immunocytochemistry to determine the impact of a prolonged activity increase on
10 gephyrin and $\alpha 2$ GABA_AR clustering (Fig. 4A). Quantification across independent
11 experiments showed that fluorescence intensity of eGFP-WT gephyrin clusters
12 increased by 1.95 fold after 8 h and by 2.3 fold after 48 h of 4-AP treatment (Fig. 4B).
13 Quantification for $\alpha 2$ GABA_AR cluster intensity after 8 h of 4-AP induced neuronal
14 activity did not show an increase in receptor accumulation at synapses; however, after
15 48 h of 4-AP treatment we found a 1.7 fold increase in receptor density at synaptic sites
16 (Fig. 4C). Thus, gephyrin recruitment at synapses precedes that of the receptor in
17 response to chronic changes in activity. In contrast to synaptic clusters, extrasynaptic
18 $\alpha 2$ clusters decreased in size and intensity after 8 h of 4-AP application (Fig. 4D). This
19 transient decrease in extrasynaptic $\alpha 2$ clusters intensity is reversed after 48 h of 4-AP
20 similar to synaptic receptor clusters (Fig. 4C-D). Therefore, a chronic increase in
21 activity regulates both extrasynaptic and synaptic receptor clustering.

22 It has been reported that acute 4-AP treatment increases GABA_AR mobility between
23 synaptic and extrasynaptic sites (Bannai et al., 2009). Hence, we analyzed $\alpha 2$ GABA_AR
24 surface diffusion at extrasynaptic and synaptic sites after either 8 h or 48 h of 4-AP
25 treatment using QD-SPT (Fig. 4E). Quantification of the receptor diffusion coefficient

1 showed a 1.3 fold reduction for extrasynaptic receptors; however, the synaptic receptors
2 were not influenced by 8 h of 4-AP treatment (Fig. 4F). Consistently, 8 h of 4-AP
3 treatment reduced the explored area for only the extrasynaptic receptors by 1.2 fold
4 (Fig. 4G). The receptor dwell time at synaptic sites was also unchanged after 8 h of
5 activity change (Fig. 4H). This is consistent with a lack of receptor accumulation at
6 synapses after 8 h of 4-AP treatment.

7 Contrary to the 8 h 4-AP treatment, 48 h treatment significantly reduced the diffusion
8 coefficients of synaptic $\alpha 2$ receptors by 1.3 fold, while having no effect on the
9 extrasynaptic receptors (Fig. 4I). We also observed a 1.3 fold reduction in explored area
10 for synaptic $\alpha 2$ GABA_ARs, with only a modest reduction for extrasynaptic receptors
11 (Fig. 4J). Unexpectedly, the reduction in the diffusion rate and explored area of synaptic
12 $\alpha 2$ receptors had no influence on the dwell time at synaptic sites (Fig. 4K). Therefore,
13 pools of extrasynaptic and synaptic receptor are regulated independently of each other
14 over prolonged activity change.

15 Altogether, our data show that GABA_AR lateral diffusion can be regulated on a time
16 scale of days. We observe a decrease in synaptic GABA_AR diffusion at 48 h time point
17 and not at 8 h, which is in direct correlation to cluster intensity change observed after
18 48 h. Therefore, regulation of GABA_AR diffusion capture accounts for the change in
19 receptor density at synapses upon chronic changes in activity.

20

21 **PKA and CaMKII α pathways regulate synaptic scaling at GABAergic** 22 **postsynaptic sites through gephyrin phosphorylation.**

23 To identify signaling cascades which couple the gephyrin scaffold to GABA_ARs for
24 activity-dependent synaptic recruitment, we focused on the PKA and CaMKII α
25 pathways. NMDA receptor dependent compensatory adaptations at the GABAergic

1 postsynaptic sites have been reported to be facilitated by gephyrin phosphorylation at
2 PKA and CaMKII α locations (Flores et al., 2015). We thus transfected the eGFP-
3 S303A/S305A (SSA) mutant (insensitive to PKA and CaMKII α dependent
4 phosphorylation) into our primary hippocampal neurons and treated the neurons for 8h
5 or 48h with 4-AP. We did not observe differences between eGFP-WT and eGFP-SSA
6 cluster number, cluster size and fluorescence intensity in control conditions (Fig. 5B).
7 Similarly, the SSA mutant did not significantly influence the synaptic or extrasynaptic
8 clustering of α 2 GABA_ARs (Fig. 5B). In contrast, the SSA mutation increased the
9 diffusion coefficient and explored area of α 2 GABA_ARs at both extrasynaptic and
10 synaptic sites (Fig. 5C-D). This increase in receptor mobility did not correlate with what
11 we expected from a normal size scaffold. However, the α 2 GABA_ARs dwell time at
12 inhibitory synapses did not differ between eGFP-SSA and eGFP-WT transfected
13 neurons (Fig. 5E), indicating that the increase in receptor mobility was not accompanied
14 by a faster synaptic escape of receptors. This is consistent with a lack of effect of the
15 SSA mutant on α 2 GABA_ARs clustering at synapses.

16 The expression of the eGFP-SSA mutant was sufficient to prevent the 4-AP (8 h or 48
17 h) induced gephyrin and α 2 GABA_ARs cluster growth at synapses (Fig. 5A, F-G).
18 Interestingly, 8 h and 48 h post 4-AP application extrasynaptic α 2 cluster intensity
19 increased in eGFP-SSA transfected neurons (Fig. 5H). This indicated that receptor
20 clustering at extrasynaptic sites at the 8 h treatment time point is dependent on PKA
21 and CaMKII α phosphorylation. However, at 48 h receptor accumulation is independent
22 of these two pathways. Hence, an additional pathway permits GABA_AR recruitment, in
23 particular at extrasynaptic sites, after chronic changes in activity.

24 We also analyzed the effect of the SSA mutant on α 2 GABA_ARs surface diffusion.
25 Similar to wild-type gephyrin, SSA reduced diffusion coefficient and surface

1 exploration of $\alpha 2$ GABA_ARs at extrasynaptic sites after 8 h of 4-AP (Fig. 5I-J). This
2 effect was maintained also after 48 h treatment (Fig. 5K-L). In contrast to wild-type
3 gephyrin, SSA mutant increased $\alpha 2$ GABA_AR confinement, and decreased resident
4 time of GABA_ARs at synapses after 48 h of 4-AP (Fig. 5K-M). The passing $\alpha 2$
5 GABA_ARs remained unchanged at synapses after 8 h or 48 h of 4-AP (Fig. 5M). Hence,
6 our results indicate that gephyrin scaffold reorganization via PKA and CaMKII α
7 dependent phosphorylation at S303 and S305 is essential for GABA_AR diffusion at
8 synapses but not at extrasynaptic sites in response to chronic changes in activity.

9

10 **Synapse scaling is independent of ERK1/2 pathway.**

11 It has been reported that gephyrin clustering is also influenced by ERK1/2 pathway.
12 We thus assessed if ERK1/2 signaling influences gephyrin cluster size during chronic
13 changes in network activity. Transgenic expression of eGFP-S268E gephyrin mutant
14 renders gephyrin scaffold insensitive to the ERK1/2 signaling pathway (Tyagarajan et
15 al., 2013). We therefore transfected cultured neurons with eGFP-S268E mutant and
16 treated them with 4-AP for 8 h or 48 h. Immunocytochemical analysis showed an
17 increase in eGFP-S268E mutant cluster size after 4-AP treatment (Fig. 6A).
18 Quantification of changes in eGFP-S268E cluster intensity confirmed an increase of
19 1.6 and 2.2 fold after 8 h and 48 h of 4-AP treatment respectively (Fig. 6B). This was
20 associated with increases of 1.2 and 1.3 fold in eGFP-S268E cluster size after 8 h and
21 48 h of 4-AP treatment respectively (Fig. 6B). Analysis for $\alpha 2$ GABA_AR cluster
22 intensity at synapses and at extrasynaptic sites showed a respective 2.2 and 1.8 fold
23 increase after 48 h of 4-AP treatment, but not after 8 h (Fig. 6C-D). We conclude that
24 the eGFP-S268E mutant is not required for the activity-dependent recruitment of
25 gephyrin and GABA_AR within synaptic and extrasynaptic clusters. We wondered if 4-

1 AP induced chronic activity would impact the surface diffusion of GABA_ARs. We
2 checked $\alpha 2$ GABA_AR diffusion coefficients after 8 h or 48 h of 4-AP. Individual
3 receptor trajectories for extrasynaptic and synaptic $\alpha 2$ GABA_AR suggested increased
4 confinement after 48 h of enhanced activity (Fig. 6E). The $\alpha 2$ diffusion coefficients
5 and explored area were increased by 1.2 fold and 1.4 fold for extrasynaptic receptors
6 after 8 h of 4-AP (Fig. 6F-G). However, 48 h post 4-AP application extrasynaptic
7 receptors diffusion coefficients were unchanged (Fig 6H), while QDs were more
8 confined at extrasynaptic sites (Fig. 6I). Interestingly, 48 h of 4-AP treatment reduced
9 synaptic $\alpha 2$ GABA_AR diffusion coefficients and explored area at eGFP-S268E
10 synapses (Fig. 6H-I) as observed at synapses containing eGFP-WT (Fig. 4I-J). In
11 agreement with an increased number of $\alpha 2$ GABA_ARs at synapses, $\alpha 2$ dwell time
12 increased at eGFP-S268E synapses (Fig. 6J).

13 Therefore, we conclude that although ERK1/2 signaling is not necessary for the
14 activity-dependent regulation of the diffusive behavior of synaptic GABA_ARs, it
15 controls the mobility of receptors at extrasynaptic sites. These observations further
16 confirm that synaptic and extrasynaptic receptor pools are independently regulated, and
17 that adaptations observed at GABAergic postsynapses is independent of ERK1/2
18 pathway.

19

20 **GSK3 β phosphorylation of gephyrin facilitates GABA_AR diffusion after activity**
21 **change.**

22 It has been reported that the GSK3 β signaling pathway postsynaptically regulates the
23 density and size of GABAergic synapses via gephyrin phosphorylation.
24 Pharmacological blockade of the GSK3 β pathway or expression of the S270A gephyrin
25 mutant is sufficient to increase gephyrin cluster size (Tyagarajan et al., 2011). Hence,

1 it is plausible that GSK3 β pathway acts in addition to PKA and CaMKII α signaling to
2 regulate homeostatic adaptations at GABAergic synapses. To address this question, we
3 treated neurons transfected with eGFP-S270A gephyrin mutant with 4-AP for 8 h and
4 48 h. Morphological characterization showed that the GSK3 β signaling is not essential
5 for gephyrin accumulation at synapses upon chronic changes in activity (Fig. 7A-B). In
6 contrast, the eGFP-S270A mutant fully abolished the synaptic and extrasynaptic
7 increase in α 2 GABA_AR clustering after 48 h of 4-AP application (Fig. 7C-D). After
8 8h of 4-AP treatment extrasynaptic α 2 GABA_AR cluster density, size and intensity
9 were respectively reduced by 1.4 fold, 1.2 fold and 1.4 fold in eGFP-S270A expressing
10 cells, respectively (Fig. 7D). These results implicate the GSK3 β pathway in the
11 regulation of activity-induced GABA_AR clustering at both synaptic and extrasynaptic
12 sites.

13 If the GSK3 β signaling is important for GABA_ARs accumulation at synapses in
14 response to chronic changes in activity, then eGFP-S270A mutant expression should
15 have no impact on α 2 diffusion rates. However, 8 h post 4-AP application α 2 diffusion
16 coefficient and explored area were reduced by 1.3 fold and 1.1 fold at synaptic sites
17 (Fig. 7E-G). This increased confinement was counterbalanced by a decrease in the time
18 trapped receptors spent at synapses (Fig. 7J), explaining why α 2 clustering was
19 unchanged at synapses after 8 h of 4-AP application. On the other hand, 48 h of 4-AP
20 application increased α 2 diffusion coefficients by 1.3 fold as well as explored area at
21 synaptic sites (Fig. 7E, H-I). This was however not accompanied by a change in
22 synaptic receptor dwell time (Fig. 7J). The reduction of extrasynaptic α 2 clustering
23 coincided with a 1.3 fold reduced explored area in eGFP-S270A expressing cells after
24 8 h of 4-AP (Fig. 7E-G). Nevertheless, 48 h after 4-AP application α 2 diffusion
25 coefficients and explored area returned to baseline levels at extrasynaptic sites (Fig.

1 7H-I). These observations are consistent with the receptor clustering returning to
2 control levels at extrasynaptic sites after 48 h of 4-AP (Fig. 7D). Altogether, these
3 results show that GSK3 β signaling in addition to PKA and CaMKII α pathways tune
4 GABA_ARs at synapses in response to chronic changes in activity.

5

6 **Impairment of PKA, CAMKII α and GSK3 β phosphorylation of gephyrin abolishes**
7 **the activity-dependent regulation of GABA_ARs mobility.**

8 The analysis of the SSA and S270A mutants indicated that PKA, CAMKII α and
9 GSK3 β phosphorylation of gephyrin have complementary effects on gephyrin and α 2
10 GABA_ARs clustering in conditions of synaptic plasticity. To show it more directly, we
11 generated eGFP-SSA/S270A mutant, expressed it in hippocampal neurons and treated
12 the neurons for 8 h or 48 h with 4-AP.

13 We found that overexpressing eGFP-SSA/S270A increased eGFP cluster size and
14 intensity (Fig. 8A). The gephyrin cluster growth was however not accompanied by
15 synaptic recruitment of α 2 GABA_ARs (Fig. 8A). Although the density of α 2 GABA_ARs
16 clusters was reduced in eGFP-SSA/S270A transfected cells, there was no major impact
17 of the mutant on α 2 GABA_ARs cluster size and intensity at synaptic and extrasynaptic
18 sites (Fig. 8A).

19 We then characterized α 2 GABA_AR diffusion in SSA/S270A transfected neurons.
20 Diffusion coefficients showed a 1.4 fold increase for extrasynaptic receptors and no
21 significant change for synaptic receptors (Fig. 8B). This effect was consistent with the
22 observation that α 2 GABA_AR spent the same time at eGFP-SSA/S270A and eGFP-WT
23 synapses (Fig. 8C). Therefore the eGFP-SSA/S270A mutant can recapitulate many of
24 the observed phenotypes seen with SSA or S270A individual mutations.

1 We then characterized how chronic activity impacts eGFP-SSA/S270A mutant
2 behavior. Although the extrasynaptic GABA_ARs cluster density increased after 48 h of
3 4-AP in eGFP-SSA/S270A transfected cells, the triple mutant prevented the synaptic
4 increase in gephyrin and GABA_ARs cluster size and intensity in response to 4-AP
5 treatment (Fig. 8D-F). The diffusion coefficient and explored area of $\alpha 2$ GABA_ARs
6 showed no change after 8 h or 48 h of 4-AP application (Fig. 8 G-J). There was also no
7 impact on receptor dwell time at synapses after chronic changes in activity (Fig. 8K).
8 Our results uncover a role for several signaling pathways in chronic activity-dependent
9 modulation of gephyrin clustering and GABA_ARs surface diffusion at synapses. Our
10 data also show that distinct signaling pathways regulate synaptic and extrasynaptic
11 receptors clustering. Together these results identify a novel role of GSK3 β signaling in
12 the regulation of extrasynaptic receptor surface trafficking and GSK3 β , PKA and
13 CaMKII α pathways in facilitating adaptations of synaptic receptors.

14

15

16 **Discussion:**

17 In the current study, we investigate the molecular basis for gephyrin scaffold induced
18 GABA_AR membrane dynamics. We identify a novel role for gephyrin post-translational
19 modification involving phosphorylation and de-phosphorylation in regulating
20 GABA_AR lateral diffusion. By tracking $\alpha 2$ GABA_ARs within and outside synaptic sites
21 using QD-SPT, we demonstrate that gephyrin phosphorylation by ERK1/2 at S268, and
22 inhibition of GSK3 β phosphorylation on gephyrin at S270 while exhibiting opposite
23 effects on synaptic morphology, influence GABA_AR diffusion properties similarly. We
24 analyze gephyrin scaffold organization at the nanoscale level using PALM, and uncover
25 that phosphorylation also controls gephyrin molecule packing.

1 Over the past decade, several independent studies have documented changes in lateral
2 diffusion of GABA_ARs after pharmacological alteration of neuronal function within a
3 time scale of minutes to few hours (Lévi et al., 2008; Bannai et al., 2009; Niwa et al.,
4 2012; Petrini et al., 2014). 4-AP application within minutes induces NMDAR-mediated
5 calcium influx and calcineurin activation leading to dephosphorylation of the GABA_AR
6 γ 2 subunit S327 residue (Wang et al., 2003). In this context, an increase in GABA_AR
7 diffusion constraint results from receptor dephosphorylation, while gephyrin scaffold
8 loss is a secondary effect in response to receptor dispersal (Niwa et al., 2012). We
9 identify gephyrin phosphorylation as an essential facilitator of GABA_AR diffusion
10 dynamics in response to chronic changes in activity. More specifically we identify a
11 central role for PKA and CaMKII α pathways along with GSK3 β signaling in
12 phosphorylating gephyrin to regulate activity-dependent inhibitory synapse
13 remodeling.

14

15 **Structure of the gephyrin scaffold requires phosphoregulation of gephyrin**
16 **molecules.**

17 At GABAergic synapses the role of phosphorylation for gephyrin scaffold
18 compaction have yet to be reported. The fluorescence microscopy data (Figure 1B)
19 inform us about average area and intensity per cluster. PALM microscopy informs us
20 about the actual density of molecules per surface area (Figure 3). The number of
21 molecules per synapse using PALM imaging can be roughly estimated by multiplying
22 the mean surface area of the cluster by the density of gephyrin molecules per surface
23 unit. Values of ~ 212, 156 and 220 were found for the gephyrin WT, S268E and S270A
24 respectively. Interestingly, these estimations are consistent with the measurements of
25 the mean cluster fluorescence intensity for the S268E and S270A mutants.

1 The hexameric gephyrin lattice model was proposed based on G and E domain crystal
2 structures available at the time. However, in recent years atomic force microscopy
3 (AFM) and small-angle X-ray scattering (SAXS) structure of full-length gephyrin has
4 shown that gephyrin only exist as trimers, as individual E domains are in an open
5 extended confirmation (Sander et al., 2013). (Pennacchietti et al., 2017) have shown
6 that after iLTP gephyrin reorganizes itself into distinct subsynaptic nanodomains. Full-
7 length gephyrin can exist in open or closed confirmations based on the linker domain
8 folding (Sander et al., 2013). All the gephyrin phosphorylation sites have been
9 mapped to the linker domain suggesting phosphorylation is a strong candidate for
10 determining open and closed states within gephyrin nanodomains. This could in turn
11 determine the distance between two nanodomains and/or total number of nanodomains
12 within a given synapse.

13

14 **Gephyrin-independent GABA_AR adaptations at synaptic sites.**

15 It has long been assumed that alterations in GABA_AR and/or gephyrin cluster intensity
16 is indicative of the number of molecules found at the synapse, and thereby a direct
17 correlate for changes in synapse structure and function. Here we report that disrupting
18 gephyrin scaffold via the expression of the eGFP-DN mutant does not increase the
19 diffusion properties of GABA_ARs at synaptic sites. This observation was unexpected
20 as loss of the scaffolding apparatus should have increased receptor diffusion also at
21 synaptic sites. It has been reported that eGFP-DN expression significantly reduces
22 mIPSC amplitude and frequency, without leading to a complete loss of GABAergic
23 synaptic transmission (Ghosh et al., 2016). Our observation suggests that a pool of
24 gephyrin independent GABA_ARs are present in neurons. Recently,
25 GIT1/βPIX/Rac1/PAK signaling pathway was shown to contribute to GABAergic

1 transmission. β PIX is a GEF for Rac1 activating PAK, and contributing to GABA_AR
2 stability (Smith et al., 2014). Similar signaling mechanisms could be operational even
3 in the absence of gephyrin scaffold to maintain the membrane pool of GABA_ARs.

4

5 **Independent behavior of GABA_ARs at synaptic and extrasynaptic sites.**

6 Postsynaptic receptor trapping is adaptable depending on phosphorylation events that
7 impinge on scaffold-scaffold or receptor-scaffold interactions (Choquet and Triller,
8 2013). It became clear with the development of SPT approaches that receptors are also
9 hindered in their diffusion outside synapses via molecular crowding but also through
10 specific protein-protein interactions. A receptor-gephyrin interaction outside inhibitory
11 synapses has been reported earlier (Ehrensperger et al., 2007). GABA_ARs also
12 colocalize and interact with clathrin-enriched endocytic zones (EZs) that are mostly
13 localized extrasynaptically (Smith et al., 2012). Receptors in EZs don't necessarily
14 undergo internalization. They can be part of a reserve pool of receptors rapidly available
15 upon increase in synaptic activity (Petrini et al., 2014). Conversely, the GABA_AR-AP2
16 interaction within EZs has been shown to indirectly control receptor mobility and
17 number at synapses (Smith et al., 2012).

18 However, our data show independent behavior of GABA_ARs at synaptic and
19 extrasynaptic sites. After 8 h of 4-AP treatment α 2 GABA_ARs were confined at
20 extrasynaptic sites without influencing the diffusion property of synaptic receptors. In
21 contrast, after 48 h of 4-AP treatment α 2 GABA_AR confinement at extrasynaptic sites
22 was lifted, and this was followed by an increase in receptor confinement at synapses,
23 suggesting that GABA_AR retention at extrasynaptic sites prevent their synaptic
24 capture/accumulation. However, after 8 h of 4-AP treatment neurons expressing eGFP-
25 S268E mutant show a reduction in receptor confinement at extrasynaptic locations,

1 without affecting synaptic receptor diffusion. Therefore, removing diffusion constraints
2 onto extrasynaptic GABA_ARs does not facilitate receptor recruitment at synapses. In
3 addition, after 8 h of 4-AP treatment neurons expressing eGFP-S270A mutant show
4 increased confinement of GABA_ARs at both extrasynaptic and synaptic locations,
5 indicating that confining GABA_ARs at extrasynaptic locations does not prevent
6 diffusion-capture of receptors.

7

8 **Synaptic adaptation is facilitated by gephyrin phosphorylation.**

9 We present evidence for a biphasic model for activity-dependent plasticity at
10 GABAergic postsynapse. Acute 4-AP treatment increases and chronic 4-AP treatment
11 decreases $\alpha 2$ GABA_AR lateral diffusion. The observed increase in GABA_AR diffusion
12 after acute 4-AP treatment can be explained by increase in synaptic escape of receptors
13 leading to reduced postsynaptic clustering and dispersal of gephyrin molecules away
14 from the synapse (Bannai et al., 2009). On the contrary, we show here that chronic 4-
15 AP treatment leads to synaptic immobilization and recruitment of GABA_AR $\alpha 2$ and
16 gephyrin. These discrepancies are probably due to the distinct signaling pathways
17 activated by the acute and chronic changes in activity. Short term 4-AP application
18 induces NMDAR-mediated calcium influx and calcineurin activation leading to
19 dephosphorylation of GABA_AR $\gamma 2$ subunit S327 residue (Bannai et al., 2009). In this
20 context, the relief in GABA_AR diffusion constraints arises from receptor
21 dephosphorylation while gephyrin loss is a consequence of receptor dispersal (Niwa et
22 al. 2012). In contrast, we show that chronic changes in activity impacts first the
23 recruitment of gephyrin at synapses, and then allows the recruitment of GABA_ARs.
24 PKA and CaMKII α signaling act downstream of NMDAR to facilitate compensatory
25 postsynaptic adaptations at GABAergic synapses (Flores et al., 2015). Our data extends

1 this understanding by demonstrating a role for the GSK3 β pathway in addition to PKA
2 and CaMKII α pathways in facilitating gephyrin scaffold organization of individual
3 GABA_ARs after prolonged changes in activity.

4

5 **References:**

6 Bannai H, Lévi S, Schweizer C, Inoue T, Launey T, Racine V, Sibarita J-B, Mikoshiba
7 K, Triller A (2009) Activity-dependent tuning of inhibitory neurotransmission
8 based on GABAAR diffusion dynamics. *Neuron* 62:670–682.

9 Bannai H, Niwa F, Sherwood MW, Shrivastava AN, Arizono M, Miyamoto A, Sugiura
10 K, Lévi S, Triller A, Mikoshiba K (2015) Bidirectional Control of Synaptic
11 GABAAR Clustering by Glutamate and Calcium. *Cell Rep* 13:2768–2780.

12 Bats C, Groc L, Choquet D (2007) The interaction between Stargazin and PSD-95
13 regulates AMPA receptor surface trafficking. *Neuron* 53:719–734.

14 Chamma I, Heubl M, Chevy Q, Renner M, Moutkine I, Eugène E, Poncer JC, Lévi S
15 (2013) Activity-dependent regulation of the K/Cl transporter KCC2 membrane
16 diffusion, clustering, and function in hippocampal neurons. *J Neurosci* 33:15488–
17 15503.

18 Charrier C, Machado P, Tweedie-Cullen RY, Rutishauser D, Mansuy IM, Triller A
19 (2010) A crosstalk between β 1 and β 3 integrins controls glycine receptor and
20 gephyrin trafficking at synapses. *Nat Neurosci* 13:1388–1395.

21 Chen JL, Villa KL, Cha JW, So PTC, Kubota Y, Nedivi E (2012) Clustered dynamics
22 of inhibitory synapses and dendritic spines in the adult neocortex. *Neuron* 74:361–
23 373.

- 1 Choquet D, Triller A (2013) The dynamic synapse. *Neuron* 80:691–703.
- 2 Ehrensperger M-V, Hanus C, Vannier C, Triller A, Dahan M (2007) Multiple
3 association states between glycine receptors and gephyrin identified by SPT
4 analysis. *Biophysical Journal* 92:3706–3718.
- 5 Flores CE, Nikonenko I, Mendez P, Fritschy J-M, Tyagarajan SK, Muller D (2015)
6 Activity-dependent inhibitory synapse remodeling through gephyrin
7 phosphorylation. *Proceedings of the National Academy of Sciences* 112:E65–E72.
- 8 Ghosh H, Auguadri L, Battaglia S, Simone Thirouin Z, Zemoura K, Messner S, Acuña
9 MA, Wildner H, Yévenes GE, Dieter A, Kawasaki H, O Hottiger M, Zeilhofer HU,
10 Fritschy J-M, Tyagarajan SK (2016) Several posttranslational modifications act in
11 concert to regulate gephyrin scaffolding and GABAergic transmission. *Nat*
12 *Commun* 7:13365.
- 13 Lardi-Studler B, Smolinsky B, Petitjean CM, Koenig F, Sidler C, Meier JC, Fritschy
14 JM, Schwarz G (2007) Vertebrate-specific sequences in the gephyrin E-domain
15 regulate cytosolic aggregation and postsynaptic clustering. *J Cell Sci* 120:1371–
16 1382.
- 17 Lévi S, Schweizer C, Bannai H, Pascual O, Charrier C, Triller A (2008) Homeostatic
18 regulation of synaptic GlyR numbers driven by lateral diffusion. *Neuron* 59:261–
19 273.
- 20 Lüscher B, Fuchs T, Kilpatrick CL (2011) GABAA receptor trafficking-mediated
21 plasticity of inhibitory synapses. *Neuron* 70:385–409.
- 22 Muir J, Arancibia-Carcamo IL, MacAskill AF, Smith KR, Griffin LD, Kittler JT (2010)

1 NMDA receptors regulate GABAA receptor lateral mobility and clustering at
2 inhibitory synapses through serine 327 on the $\gamma 2$ subunit. *Proceedings of the*
3 *National Academy of Sciences* 107:16679–16684.

4 Niwa F, Bannai H, Arizono M, Fukatsu K, Triller A, Mikoshiba K (2012) Gephyrin-
5 independent GABA(A)R mobility and clustering during plasticity. *PLoS ONE*
6 7:e36148.

7 Pennacchietti F, Vascon S, Nieuw T, Rosillo C, Das S, Tyagarajan SK, Diaspro A, Del
8 Bue A, Petrini EM, Barberis A, Cella Zanacchi F (2017) Nanoscale Molecular
9 Reorganization of the Inhibitory Postsynaptic Density Is a Determinant of
10 GABAergic Synaptic Potentiation. *J Neurosci* 37:1747–1756.

11 Petrini EM, Barberis A (2014) Diffusion dynamics of synaptic molecules during
12 inhibitory postsynaptic plasticity. *Front Cell Neurosci* 8:300.

13 Petrini EM, Ravasenga T, Hausrat TJ, Jurilli G, Olcese U, Racine V, Sibarita J-B, Jacob
14 TC, Moss SJ, Benfenati F, Medini P, Kneussel M, Barberis A (2014) Synaptic
15 recruitment of gephyrin regulates surface GABAA receptor dynamics for the
16 expression of inhibitory LTP. *Nat Commun* 5.

17 Rannals MD, Kapur J (2011) Homeostatic strengthening of inhibitory synapses is
18 mediated by the accumulation of GABA(A) receptors. *J Neurosci* 31:17701–
19 17712.

20 Renner M, Schweizer C, Bannai H, Triller A, Lévi S (2012) Diffusion Barriers
21 Constrain Receptors at Synapses Tell F, ed. *PLoS ONE* 7:e43032.

22 Saliba RS, Michels G, Jacob TC, Pangalos MN, Moss SJ (2007) Activity-dependent

1 ubiquitination of GABA(A) receptors regulates their accumulation at synaptic
2 sites. *J Neurosci* 27:13341–13351.

3 Sander B, Tria G, Shkumatov AV, Kim EY, Grossmann JG, Tessmer I, Svergun DI,
4 Schindelin H (2013) Structural characterization of gephyrin by AFM and SAXS
5 reveals a mixture of compact and extended states. *Acta Crystallogr D Biol*
6 *Crystallogr* 69:2050–2060.

7 Smith KR, Davenport EC, Wei J, Li X, Pathania M, Vaccaro V, Yan Z, Kittler JT
8 (2014) GIT1 and β PIX are essential for GABA(A) receptor synaptic stability and
9 inhibitory neurotransmission. *Cell Rep* 9:298–310.

10 Smith KR, Muir J, Rao Y, Browarski M, Gruenig MC, Sheehan DF, Haucke V, Kittler
11 JT (2012) Stabilization of GABA(A) receptors at endocytic zones is mediated by
12 an AP2 binding motif within the GABA(A) receptor β 3 subunit. *J Neurosci*
13 32:2485–2498.

14 Specht CG, Izeddin I, Rodriguez PC, Beheiry El M, Rostaing P, Darzacq X, Dahan M,
15 Triller A (2013) Quantitative nanoscopy of inhibitory synapses: counting gephyrin
16 molecules and receptor binding sites. *Neuron* 79:308–321.

17 Tyagarajan SK, Ghosh H, Yévenes GE, Imanishi SY, Zeilhofer HU, Gerrits B, Fritschy
18 J-M (2013) Extracellular signal-regulated kinase and glycogen synthase kinase 3 β
19 regulate gephyrin postsynaptic aggregation and GABAergic synaptic function in a
20 calpain-dependent mechanism. *J Biol Chem* 288:9634–9647.

21 Tyagarajan SK, Ghosh H, Yévenes GE, Nikonenko I, Ebeling C, Schwerdel C, Sidler
22 C, Zeilhofer HU, Gerrits B, Muller D, Fritschy J-M (2011) Regulation of
23 GABAergic synapse formation and plasticity by GSK3beta-dependent

1 phosphorylation of gephyrin. Proceedings of the National Academy of Sciences
2 108:379–384.

3 van Versendaal D, Rajendran R, Saiepour MH, Klooster J, Smit-Rigter L, Sommeijer
4 J-P, De Zeeuw CI, Hofer SB, Heimel JA, Levelt CN (2012) Elimination of
5 Inhibitory Synapses Is a Major Component of Adult Ocular Dominance Plasticity.
6 Neuron 74:374–383.

7 Villa KL, Berry KP, Subramanian J, Cha JW, Oh WC, Kwon H-B, Kubota Y, So PTC,
8 Nedivi E (2016) Inhibitory Synapses Are Repeatedly Assembled and Removed at
9 Persistent Sites In Vivo. Neuron 89:756–769.

10 Vlachos A, Reddy-Alla S, Papadopoulos T, Deller T, Betz H (2013) Homeostatic
11 regulation of gephyrin scaffolds and synaptic strength at mature hippocampal
12 GABAergic postsynapses. Cereb Cortex 23:2700–2711.

13 Wang J, Liu S, Haditsch U, Tu W, Cochrane K, Ahmadian G, Tran L, Paw J, Wang Y,
14 Mansuy I, Salter MM, Lu YM (2003) Interaction of calcineurin and type-A GABA
15 receptor gamma 2 subunits produces long-term depression at CA1 inhibitory
16 synapses. J Neurosci 23:826–836.

17 Yu W, Jiang M, Miralles CP, Li R-W, Chen G, De Blas AL (2007) Gephyrin clustering
18 is required for the stability of GABAergic synapses. Mol Cell Neurosci 36:484–
19 500.

20
21
22

1 **Figure Legends**

2 **Figure 1: Morphological characterization of eGFP-gephyrin and its mutant**

3 **variants. (A)** Representative images of primary hippocampal neurons co-transfected

4 with eGFP-WT, eGFP-S268E, eGFP-S270A or eGFP-DN and shRNA-3'UTR. eGFP-

5 gephyrin clusters (green), $\alpha 2$ GABA_ARs (red) and VGAT (blue) are shown. Scale bar,

6 10 μ m. **(B)** Quantification of eGFP-gephyrin cluster density, cluster area and intensity

7 shows larger eGFP-S270A clusters compared with eGFP-WT at synapses. **S268E:** WT

8 n= 66 cells, S268E n= 60 cells, 4 cultures. **Syn:** Cluster Number (Nb) p= 0.42, area p=

9 0.22, intensity (Int) p= 0.05. **Extra:** Nb p= 0.99, Area p= 0.66, Intensity p= 0.44.

10 S270A: WT n= 86 cells, **S270A:** n= 74 cells, 6 cultures. **Syn:** Nb p= 0.77, Area p=

11 0.02, Intensity p= 0.02. **Extra:** Nb p= 0.39, Area p= 0.42, Intensity p= 0.15. **(C)**

12 Quantification for $\alpha 2$ GABA_AR clusters shows significantly more receptors in eGFP-

13 S270A mutant clusters. **S268E:** WT n= 52 cells, S268E n= 47 cells, 3 cultures. **Syn:**

14 Nb p= 0.48, Area p= 0.46, Intensity p= 0.6. **Extra:** Nb p= 0.46, area p= 0.63, intensity

15 p= 0.22. **S270A:** WT n= 52 cells, S270A n= 39 cells, 3 cultures. **Syn:** Nb p= 0.56, Area

16 p= 0.08, Intensity p= 0.008. **Extra:** Nb p= 0.008, Area p= 0.81, Intensity p= 0.29. Data

17 shown as mean \pm SEM. Values were normalized to the corresponding control values.

18 Statistics *P \leq 0.05, **P \leq 0.01 (Mann Whitney Rank sum test).

19

20 **Figure 2: Membrane dynamics of $\alpha 2$ GABA_AR is influenced by gephyrin**

21 **phosphorylation. (A)** Example traces of QD trajectories (red) overlaid with fluorescent

22 synaptic clusters (white) of VGAT-Oyster550 for eGFP-DN transfected neurons or

23 with eGFP-gephyrin clusters for eGFP-WT, eGFP-S268E or eGFP-S270A expressing

24 cells. Scale bar, 0.5 μ m. **(B)** Median diffusion coefficients D of $\alpha 2$ GABA_AR in neurons

25 transfected with either eGFP-WT or eGFP-DN. **Extra:** WT n= 975 QDs, DN n= 491

1 QDs, $p= 4.5 \cdot 10^{-34}$; **Syn:** WT $n= 306$ QDs, DN $n= 173$ QDs, $p= 0.36$. **(C)** Quantification
2 of explored area EA of $\alpha 2$ GABA_AR, **Extra:** WT $n= 2925$ QDs, DN $n= 1473$ QDs, $p=$
3 $3.8 \cdot 10^{-23}$; **Syn:** WT $n= 918$ QDs, DN $n= 519$ QDs, $p= 4.4 \cdot 10^{-4}$. **(D)** Dwell time DT of
4 $\alpha 2$ GABA_AR at synapses in neurons transfected with either eGFP-WT or eGFP-DN.
5 Quantification of all QDs (total), trapped (DT < 5.9 s) and passing (DT > 5.9 s) QDs at
6 inhibitory synapses. Significant decrease in synaptic dwell time for total and trapped
7 QDs was observed but not for passing ones. **Total:** WT $n= 436$ QDs, DN $n= 262$ QDs,
8 $p= 0.001$; **Trapped:** WT $n= 235$ QDs, DN $n= 108$ QDs, $p= 8.0 \cdot 10^{-3}$; **Passing:** WT $n=$
9 201 QDs, DN $n= 154$ QDs, $p= 0.19$. **(E)** Quantification of diffusion coefficients of $\alpha 2$
10 GABA_AR showing increased receptor mobility at extrasynaptic (extra) and synaptic
11 (syn) sites in neurons transfected with eGFP-S268E or eGFP-S270A, as compared with
12 eGFP-WT expressing cells. **Extra:** WT $n= 1820$ QDs, S268E $n= 1273$ QDs, $p= 1.1 \cdot 10^{-$
13 22 , S270A $n= 1658$, $p= 2.9 \cdot 10^{-27}$. **Syn:** WT $n= 461$ QDs, S268E $n= 326$ QDs, $p= 2.4 \cdot 10^{-$
14 8 , S270A $n= 340$, $p= 1.8 \cdot 10^{-8}$. **(F)** Quantification of $\alpha 2$ GABA_AR explored area EA,
15 **Extra:** WT $n= 5460$ QDs, S268E $n= 3807$ QDs, $p= 6.8 \cdot 10^{-52}$, S270A $n= 5355$, $p= 2.2$
16 $\cdot 10^{-101}$. **Syn:** WT $n= 1383$ QDs, S268E $n= 978$ QDs, $p= 7.4 \cdot 10^{-23}$, S270A $n= 2208$, $p=$
17 $1.2 \cdot 10^{-33}$. **(G)** Quantification of $\alpha 2$ GABA_AR dwell time DT in neurons expressing
18 either eGFP-WT, eGFP-S268E or eGFP-S270A. Calculations were done for all QDs
19 (total), (trapped) or (passing) QDs at inhibitory synapses. Decrease in dwell time for
20 the whole or trapped population of QDs was seen in synapses expressing eGFP-S268E
21 but not in synapses containing eGFP-S270A. **Total:** WT $n= 251$ QDs, S268E $n= 176$
22 QDs, $p= 0.013$, S270A $n= 216$ QDs, $p= 0.31$; **Trapped:** WT $n= 135$ QDs, S268E $n=$
23 85 QDs, $p= 0.002$, S270A $n= 109$ QDs, $p= 0.28$; **Passing:** WT $n= 116$ QDs, S268E $n=$
24 91 QDs, $p= 0.24$, S270A $n= 107$ QDs, $p= 0.98$. All data are from six independent
25 experiments. In B-C, E-F, data are presented as median values $\pm 25\%$ -75% Interquartile

1 Range IQR, ***P≤0.001 (Kolmogorov-Smirnov test). In D, G, data are presented as
2 mean ± SEM. *P≤0.05, **P≤0.01 (Mann Whitney Rank sum test). D in $\mu\text{m}^2\text{s}^{-1}$, EA in
3 μm^2 , DT in s.

4

5 **Figure 3: PALM imaging showing gephyrin phosphorylation influences scaffold**
6 **packing. (A)** Epifluorescence (top) and PALM (bottom) imaging of the same dendritic
7 regions in neurons expressing pDendra2-WT, -S268E or -S270A mutant. Scale bar, 1
8 μm . **(B)** Representative image of cluster segmentation (red) based on local density of
9 molecules detected (white dots) using a threshold of 1000 detections/ μm^2 (blue). Scale
10 bar, 200 nm. **(C)** Quantification of eGFP cluster area using PALM shows reduction in
11 cluster size for eGFP-S268E and increase in cluster size for eGFP-S270A compared
12 with eGFP-WT. WT n= 313 synapses, S268E n= 277 synapses, S270A n= 290
13 synapses, p<0.001, 4 cultures. **(D)** Quantification of density of gephyrin molecules per
14 μm^2 using PALM in transfected neurons. Neurons expressing eGFP-S268E exhibit
15 denser gephyrin packing, and neurons expressing eGFP-S270A exhibit less dense
16 packing of gephyrin compared with eGFP-WT. Data are presented as mean ± SEM.
17 **P= 0.006; ***P≤0.001 (Mann Whitney Rank sum test).

18

19 **Figure 4: Gephyrin clustering influences GABA_AR lateral diffusion. (A)**
20 Morphology of eGFP-WT (green) after 8 h and 48 h of 4-AP application; VGAT (blue),
21 GABA_AR $\alpha 2$ (red) at 21 DIV. Scale bar, 10 μm . **(B)** Quantification of eGFP-WT
22 clusters after 8 h and 48 h of 4-AP application. t0 n= 55 cells, 8h n= 46 cells, 48h n=
23 55 cells, 3 cultures. **Cluster Nb:** 0-8h: p= 0.13, 0-48h: p= 0.002; **Area:** 0-8h: p= 0.5,
24 0-48h: p= 0.001; **Intensity:** 0-8h: p<0.001, 0-48h: p<0.001. **(C)** Quantification of
25 synaptic $\alpha 2$ GABA_AR clusters after 8 h and 48 h of 4-AP compared with mock treated

1 control. t0 n= 52 cells, 8h n= 43 cells, 48h n= 53 cells, 3 cultures. **Cluster Nb:** 0-8h:
2 p= 0.4, 0-48h: p= 0.3; **Area:** 0-8h: p= 0.8, 0-48h: p= 0.8; **Intensity:** 0-8h: p= 0.5, 0-
3 48h: p= 0.03. **(D)** Quantification of extrasynaptic $\alpha 2$ GABA_AR clusters after 8 h and 48
4 h of 4-AP compared with mock treated control. t0 n= 52 cells, 8h n= 43 cells, 48h n=
5 53 cells, 3 cultures. **Cluster Nb:** 0-8h: p= 0.2, 0-48h: p= 0.9; **Area:** 0-8h: p= 0.02, 0-
6 48h: p= 0.3; **Intensity:** 0-8h: p= 0.05, 0-48h: p= 0.022. **(E)** Example trace of $\alpha 2$
7 GABA_AR trajectories showing surface exploration of extrasynaptic and synaptic
8 receptors after 8 h and 48 h of 4-AP exposure. Scale bar, 0.5 μ m. **(F)** Quantification of
9 diffusion coefficients of $\alpha 2$ GABA_AR after 8 h of 4-AP exposure. **Extra;** t0 n= 450
10 QDs, WT 4AP 8h n= 961 QDs, p= $1.96 \cdot 10^{-7}$. **Syn;** t0 n= 103 QDs, 8h n= 138 QDs, p=
11 0.22; 2 cultures. **(G)** Quantification of explored area EA of $\alpha 2$ GABA_AR after 8 h of 4-
12 AP application. **Extra;** t0 n= 1347 QDs, 8h n= 5265 QDs, p= $6.4 \cdot 10^{-9}$. **Syn;** t0 n= 308
13 QDs, 8h n= 708 QDs, p= 0.63. **(H)** Quantification of synaptic dwell time DT of $\alpha 2$
14 GABA_AR showing no impact after 8 h of 4-AP for either total, trapped or passing
15 receptor population. **Total:** t0 n= 151 QDs, 8h n= 206 QDs, p= 0.073; **Trapped:** t0 n=
16 80 QDs, 8h n= 116 QDs, p= 0.36; **Passing:** t0 n= 78 QDs, 8h n= 90 QDs, p= 0.02. **(I)**
17 Quantification of diffusion coefficients of $\alpha 2$ GABA_AR after 48 h of 4-AP application.
18 **Extra:** t0 n= 777 QDs, 48h n= 174 QDs, p= 0.69. **Syn:** t0 n= 126 QDs, 48h n= 213
19 QDs, p= $1.4 \cdot 10^{-4}$. **(J)** Quantification of explored area EA of $\alpha 2$ GABA_AR after 48 h of
20 4-AP application. **Extra:** t0 n= 2331 QDs, 48h n= 5508 QDs, p= 0.045. **Syn:** t0 n= 378
21 QDs, 48h n= 717 QDs, p= $2.2 \cdot 10^{-20}$. **(K)** Quantification of $\alpha 2$ GABA_AR dwell time
22 after 48 h of 4-AP application. **Total:** t0 n= 201 QDs, 48h n= 254 QDs, p= 0.74.
23 **Trapped:** t0 n= 91 QDs, 48h n= 110 QDs, p= 0.99. **Passing:** t0 n= 110 QDs, 48h n=
24 144 QDs, p= 0.81. In B-D, H, K, data are presented as mean \pm SEM, *P \leq 0.05;
25 ***P \leq 0.001 (Mann Whitney Rank sum test). In F-G, I-J, data are presented as median

1 values \pm 25%-75% Interquartile Range IQR, * $P \leq 0.05$; *** $P \leq 0.001$ (Kolmogorov-
2 Smirnov test). In B-G and I-J, values were normalized to the corresponding control
3 values. In H, K, DT in s.

4

5 **Figure 5: PKA and CaMKII α signaling pathways regulate gephyrin clustering**
6 **and $\alpha 2$ GABA $_A$ R membrane dynamics in conditions of chronic changes of activity.**

7 **(A)** Morphological analysis of neurons transfected with eGFP-S303A/S305A (eGFP-
8 SSA) gephyrin double mutant insensitive to PKA and CaMKII α signaling pathways.
9 Double staining of VGAT (blue) and $\alpha 2$ GABA $_A$ R (red) at 21 DIV under control
10 condition (t0) or in the presence of 4-AP for 48 h. Scale bar, 10 μ m. **(B)** Quantifications
11 of synaptic eGFP-SSA clusters and synaptic ($\alpha 2$ syn) and extrasynaptic ($\alpha 2$ extra) $\alpha 2$
12 GABA $_A$ R clusters in relation to eGFP-WT show minor impact of eGFP-SSA under
13 control condition. eGFP-WT: n= 89 cells, eGFP-SSA n= 95 cells, 6 cultures. **eGFP-**
14 **SSA:** Cluster Nb: p= 0.3; Area: p= 0.9; Intensity: p= 0.5. **$\alpha 2$ syn:** Cluster Nb: p= 0.4;
15 Area: p= 0.5; Intensity: p= 0.8. **$\alpha 2$ extra:** Cluster Nb: p= 0.2; Area: p= 0.4; Intensity:
16 p= 0.2. **(C)** Quantification of median diffusion coefficient D of $\alpha 2$ GABA $_A$ R in neurons
17 expressing eGFP-WT or eGFP-SSA under control condition. **Extra:** WT n= 1166 QDs,
18 SSA n= 989 QDs, p= $1.5 \cdot 10^{-12}$; **Syn:** WT n= 312 QDs, SSA n= 245 QDs, p= 0.08; 4
19 cultures. **(D)** Quantification of median explored area EA of $\alpha 2$ GABA $_A$ R in neurons
20 expressing eGFP-WT or eGFP-SSA under control condition. **Extra:** WT n= 3510 QDs,
21 SSA n= 2778 QDs, p= $3.9 \cdot 10^{-18}$; **Syn:** WT n= 932 QDs, SSA n= 735 QDs, p= $3.1 \cdot 10^{-4}$.
22 **(E)** Quantification of $\alpha 2$ GABA $_A$ R dwell time DT at synaptic sites in neurons
23 expressing either eGFP-WT or eGFP-SSA. Calculations were done for all QDs (total),
24 (trapped) or (passing) QDs at inhibitory synapses. No significant differences were
25 found between eGFP-WT and eGFP-SSA. **Total:** WT n= 390 QDs, SSA n= 335 QDs,

1 p= 0.2; **Trapped:** WT n= 229 QDs, SSA n= 173 QDs, p= 0.4; **Passing:** WT n= 161
 2 QDs, SSA n= 162 QDs, p= 0.9. **(F)** Quantification of eGFP-SSA clusters after 8 h and
 3 48 h of 4-AP application. t0 n= 61 cells, 8h n= 52 cells, 48h n= 93 cells, 3-6 cultures.
 4 **Cluster Nb:** 0-8h: p= 0.2, 0-48h: p<0.001; **Area:** 0-8h: p= 0.8, 0-48h: p= 0.3;
 5 **intensity:** 0-8h: p= 0.8, 0-48h: p= 0.2. **(G)** Quantification of synaptic $\alpha 2$ GABA_AR
 6 clusters after 8 h and 48 h of 4-AP compared with mock treated control. t0 n= 53 cells,
 7 8h n= 50 cells, 48h n= 69 cells, 3-6 cultures. **Cluster Nb:** 0-8h: p<0.001, 0-48h:
 8 p<0.001; **Area:** 0-8h: p= 0.002, 0-48h: p= 0.09; **Intensity:** 0-8h: p= 0.5, 0-48h: p=
 9 0.5. **(H)** Quantification of extrasynaptic $\alpha 2$ GABA_AR clusters after 8 h and 48 h of 4-
 10 AP compared with mock treated control. **Cluster Nb:** 0-8h: p= 0.2, 0-48h: p= 0.1;
 11 **Area:** 0-8h: p=0.01, 0-48h: p= 0.9; **Intensity:** 0-8h: p= 0.002, 0-48h: p<0.001. **(I)**
 12 Quantification of $\alpha 2$ GABA_AR diffusion coefficients in eGFP-SSA expressing cells
 13 after 8 h of 4-AP exposure. **Extra:** t0 n= 787 QDs, 4AP 8h n= 365 QDs, p= 3.6 10⁻⁴.
 14 **Syn:** t0 n= 212 QDs, 8h n= 187 QDs, p= 0.4; 5 cultures. **(J)** Quantification of explored
 15 area EA of $\alpha 2$ GABA_AR after 8 h of 4-AP application. **Extra:** t0 n= 1869 QDs, 8h n=
 16 1092 QDs, p= 0.002. **Syn:** t0 n= 753 QDs, 8h n= 558 QDs, p= 0.09. **(K)** Quantification
 17 of $\alpha 2$ GABA_AR diffusion coefficients in eGFP-SSA expressing cells after 48 h of 4-AP
 18 exposure. **Extra:** t0 n= 1098 QDs, 4AP 48h n= 734 QDs, p= 0.002. **Syn:** t0 n= 287
 19 QDs, 48h n= 198 QDs, p= 0.2; 5 cultures. **(L)** Quantification of explored area EA of
 20 $\alpha 2$ GABA_AR after 48 h of 4-AP application. **Extra:** t0 n= 2169 QDs, 48h n= 1500 QDs,
 21 p= 0.04. **Syn;** t0 n= 633 QDs, 48h n= 510 QDs, p= 0.002. **(M)** Quantification of $\alpha 2$
 22 GABA_AR dwell time DT in neurons expressing eGFP-SSA after 8 h or 48 h of 4-AP
 23 application. Calculations were done for trapped or passing QDs at inhibitory synapses.
 24 **Trapped:** 8 h: n= 189 QDs, p= 0.3; 48 h: n= 166 QDs, p= 0.1; **Passing:** 8 h: n= 76
 25 QDs, p= 0.3; 48 h: n= 132 QDs, p= 0.9. In B, E, F-H, M, data are presented as mean \pm

1 SEM. **P<0.01; ***P≤0.001 (Mann Whitney Rank sum test). In C-D, I-L, data are
2 presented as median values ± 25%-75% IQR; ***P≤0.001 (Kolmogorov-Smirnov test).
3 In all graphs except E, values were normalized to the corresponding control values.
4
5 **Figure 6: The ERK1/2 pathway does not influence structural synaptic adaptation.**
6 **(A)** Morphological analysis of eGFP-S268E in control (t0) or after 4-AP application
7 for 8 h or 48 h. Scale bar, 10 μm. **(B)** Quantification of eGFP-S268E clusters after 8 h
8 or 48 h of 4-AP application. t0 n= 50 cells, 8h n= 54 cells, 48h n= 55 cells, 3 cultures.
9 **Cluster Nb:** 0-8h: p= 0.2, 0-48h: p= 0.004; **Area:** 0-8h: p= 0.02, 0-48h: p<0.001;
10 **intensity:** 0-8h: p=0.003, 0-48h: p<0.001. 3 cultures. **(C)** Quantification of synaptic
11 α2 GABA_AR clusters after 8 h and 48 h of 4-AP compared with mock treated control.
12 t0 n= 47 cells, 8h n= 50 cells, 48h n= 62 cells, 3-4 cultures. **Cluster Nb:** 0-8h: p= 0.08,
13 0-48h: p= 0.5; **Area:** 0-8h: p= 0.8, 0-48h: p= 0.03; **intensity:** 0-8h: p= 0.5, 0-48h:
14 p<0.001. **(D)** Quantification of extrasynaptic α2 GABA_AR clusters after 8 h and 48 h
15 of 4-AP compared with mock treated control. **Cluster Nb:** 0-8h: p= 0.006, 0-48h: p=
16 0.007; **Area:** 0-8h: p= 0.02, 0-48h: p<0.001; **intensity:** 0-8h: p= 0.04, 0-48h: p<0.001.
17 **(E)** Example traces of α2 GABA_AR trajectories at extrasynaptic (extra) and synaptic
18 (syn) sites under control condition (t0) or after 8 h or 48 h of 4-AP application. Scale
19 bar, 0.25 μm. **(F)** Quantification of α2 GABA_AR diffusion coefficients after 8 h of 4-
20 AP exposure. **Extra:** t0 n= 1230 QDs, 4AP 8h n= 1855 QDs, p= 3.4 10⁻⁶. **Syn:** t0 n=
21 281 QDs, 8h n= 378 QDs, p= 0.2; 3 cultures. **(G)** Quantification of explored area EA
22 of α2 GABA_AR after 8 h of 4-AP application. **Extra:** t0 n= 3402 QDs, 8h n= 2454 QDs,
23 p= 3.2 10⁻²³. **Syn:** t0 n= 843 QDs, 8h n= 984 QDs, p= 0.02. **(H)** Quantification of α2
24 GABA_AR diffusion coefficients after 48 h of 4-AP exposure. **Extra:** t0 n= 687 QDs,
25 4AP 48h n= 1611 QDs, p= 0.4. **Syn:** t0 n= 73 QDs, 48h n= 46 QDs, p= 1.6 10⁻⁴. **(I)**

1 Quantification of explored area EA of $\alpha 2$ GABA_AR after 48 h of 4-AP application.
2 **Extra:** t0 n= 2061 QDs, 48h n= 546 QDs, p= 2.9 10⁻⁶. **Syn;** t0 n= 219 QDs, 48h n= 74
3 QDs, p= 6.6 10⁻⁷. **(J)** Quantification of $\alpha 2$ GABA_AR dwell time DT after 8 h or 48 h of
4 4-AP application. Calculations were done for trapped or passing QDs at inhibitory
5 synapses. **Trapped:** t0: n= 130 QDs, 8 h: n= 194 QDs, p= 0.007; t0: n= 85 QDs, 48 h:
6 n= 51 QDs, p= 0.02; **Passing:** t0: n= 91 QDs, 8 h: n= 161 QDs, p<0.001; t0: n= 91
7 QDs, 48 h: n= 31 QDs, p= 0.6. In B-D, J, data are presented as mean \pm SEM. *P \leq 0.05;
8 **P \leq 0.01; ***P \leq 0.001 (Mann Whitney Rank sum test). In F-I, data are presented as
9 median values \pm 25%-75% IQR. *P \leq 0.05; ***P \leq 0.001 (Kolmogorov-Smirnov test). In
10 all graphs, values were normalized to the corresponding control values.

11

12 **Figure 7: GSK3 β pathway influences gephyrin scaffold and GABA_ARs after**
13 **changes in chronic activity. (A)** Morphology of neuron transfected with eGFP-S270A
14 under control condition (t0) or in the presence of 4-AP after 8 h or 48 h. Scale bar, 10
15 μ m. **(B)** Quantification of eGFP-S270A clusters after 8 h or 48 h of 4-AP application.
16 t0 n= 43 cells, 8h n= 50 cells; 48h n= 50 cells, 3 cultures. **Cluster Nb:** 0-8h: p= 0.8, 0-
17 48h: p= 0.14; **Area:** 0-8h: Mann Whitney test p= 0.7, 0-48h: p= 0.04; **Intensity:** 0-8h:
18 p= 0.12, 0-48h: p<0.001. **(C)** Quantification of synaptic $\alpha 2$ GABA_AR clusters after 8 h
19 and 48 h of 4-AP compared with mock treated control. t0 n= 40 cells, 8h n= 47 cells;
20 t0: n= 59 cells, 48h n= 52 cells, 3-5 cultures. **Cluster Nb:** 0-8h: p= 0.8, 0-48h: p= 0.7;
21 **Area:** 0-8h: p=0.14, 0-48h: p=0.6; **Intensity:** 0-8h: p=0.03, 0-48h: p=0.4. **(D)**
22 Quantification of extrasynaptic $\alpha 2$ GABA_AR clusters after 8 h and 48 h of 4-AP
23 compared with mock treated control. **Cluster Nb:** 0-8h: p<0.001, 0-48h: p=0.7; **Area:**
24 0-8h: p<0.001, 0-48h: p=0.7; **Intensity:** 0-8h: p<0.001, 0-48h: p=0.3. **(E)** Example
25 traces of $\alpha 2$ GABA_AR trajectories at extrasynaptic (extra) and synaptic (syn) sites under

1 control conditions (t0) or after 8 h or 48 h of 4-AP application. Scale bar, 0.25 μm . **(F)**
2 Quantification of $\alpha 2$ GABA_AR diffusion coefficients after 8 h of 4-AP exposure. **Extra:**
3 t0 n= 1580 QDs, 4AP 8h n= 1892 QDs, p= $1.4 \cdot 10^{-13}$. **Syn:** t0 n= 229 QDs, 8h n= 307
4 QDs, p= $8.8 \cdot 10^{-3}$; 3 cultures. **(G)** Quantification of explored area EA of $\alpha 2$ GABA_AR
5 after 8 h of 4-AP application. **Extra:** t0 n= 4575 QDs, 8h n= 4041 QDs, p= 0.02. **Syn:**
6 t0 n= 687 QDs, 8h n= 663 QDs, p= 0.04. **(H)** Quantification of $\alpha 2$ GABA_AR diffusion
7 coefficients after 48 h of 4-AP exposure. **Extra:** t0 n= 314 QDs, 4AP 48h n= 338 QDs,
8 p= 0.05. **Syn:** t0 n= 46 QDs, 48h n= 51 QDs, p= 0.04. 3 cultures. **(I)** Quantification of
9 explored area EA of $\alpha 2$ GABA_AR after 48 h of 4-AP application. **Extra:** t0 n= 939
10 QDs, 48h n= 771 QDs, p= 0.02. **Syn:** t0 n= 138 QDs, 48h n= 153 QDs, p= 0.04. **(J)**
11 Quantification of $\alpha 2$ GABA_AR dwell time DT after 8 h or 48 h of 4-AP application.
12 Calculations were done for trapped or passing QDs at inhibitory synapses. **Trapped:**
13 t0: n= 82 QDs, 8 h: n= 97 QDs, p= 0.04; t0: n= 191 QDs, 48 h: n= 45 QDs, p= 0.5;
14 **Passing:** t0: n= 104 QDs, 8 h: n= 131 QDs, p= 0.5; t0: n= 211 QDs, 48 h: n= 23 QDs,
15 p= 0.1. In B-D, J, data are presented as mean \pm SEM. *P \leq 0.05; ***P \leq 0.001 (Mann
16 Whitney Rank sum test). In F-I, data are presented as median values \pm 25%-75% IQR.
17 *P \leq 0.05; **P \leq 0.01; ***P \leq 0.001 (Kolmogorov-Smirnov test). In all graphs, values
18 were normalized to the corresponding control values.

19

20 **Figure 8: PKA, CAMKII α and GSK3 β pathways are required to tune the**
21 **inhibitory synapse.**

22 **(A)** Quantifications of synaptic eGFP-SSA/S270 clusters and synaptic ($\alpha 2$ syn) and
23 extrasynaptic ($\alpha 2$ extra) $\alpha 2$ GABA_AR clusters in relation to eGFP-WT show minor
24 impact of the mutant under control condition. eGFP-WT n= 58 cells, eGFP-SSA/S270A
25 n= 62 cells, 3 cultures. eGFP-SSA: **Cluster Nb:** p= 0.6; **Area:** p= 0.1; **Intensity:** p=

1 0.7. $\alpha 2$ syn: **Cluster Nb**: $p=0.001$; **Area**: $p=0.1$; **Intensity**: $p=0.02$. $\alpha 2$ extra: Cluster
2 Nb: $p=0.03$; **Area**: $p=0.5$; **Intensity**: $p=0.2$. **(B)** Quantification of median diffusion
3 coefficient D of $\alpha 2$ GABA_AR in neurons expressing eGFP-WT or eGFP-SSA/S270A
4 under control condition. **Extra**: WT $n=823$ QDs, SSA/S270A $n=786$ QDs, $p=0.004$;
5 **Syn**: WT $n=261$ QDs, SSA/S270A $n=211$ QDs, $p=0.3$, 2 cultures. **(C)** Quantification
6 of $\alpha 2$ GABA_AR dwell time DT at synaptic sites in neurons expressing either eGFP-WT
7 or eGFP-SSA/S270A. Calculations were done for all QDs (total), (trapped) or (passing)
8 QDs at inhibitory synapses. No significant differences were found between eGFP-WT
9 and eGFP-SSA/S270A. **Total**: WT $n=165$ QDs, SSA/S270A $n=183$ QDs, $p=0.1$;
10 **Trapped**: WT $n=95$ QDs, SSA/S270A $n=116$ QDs, $p=0.5$; **Passing**: WT $n=70$ QDs,
11 SSA/S270A $n=67$ QDs, $p=0.2$. **(D)** Quantification of eGFP-SSA/S270A clusters after
12 8 h or 48 h of 4-AP application. t_0 $n=53$ cells, 8h $n=45$ cells, 48h $n=51$ cells, 3
13 cultures. **Cluster Nb**: 0-8h: $p=0.3$, 0-48h: $p<0.001$; **Area**: 0-8h: $p=0.03$, 0-48h: $p=$
14 0.2 ; **Intensity**: 0-8h: $p=0.3$, 0-48h: $p=0.9$. **(E)** Quantification of synaptic $\alpha 2$ GABA_AR
15 clusters after 8 h and 48 h of 4-AP compared with mock treated control. t_0 $n=49$ cells,
16 8h $n=49$ cells, 48h $n=39$ cells, 3 cultures. **Cluster Nb**: 0-8h: $p=0.2$, 0-48h: $p<0.001$;
17 **Area**: 0-8h: $p=0.8$, 0-48h: $p=0.6$; **Intensity**: 0-8h: $p=0.2$, 0-48h: $p=0.9$. **(F)**
18 Quantification of extrasynaptic $\alpha 2$ GABA_AR clusters after 8 h and 48 h of 4-AP
19 compared with mock treated control. **Cluster Nb**: 0-8h: $p=0.8$, 0-48h: $p=0.001$; **Area**:
20 0-8h: $p<0.001$, 0-48h: $p=0.7$; **Intensity**: 0-8h: $p=0.8$, 0-48h: $p=0.8$. **(G)**
21 Quantification of $\alpha 2$ GABA_AR diffusion coefficients after 8 h of 4-AP exposure. **Extra**:
22 t_0 $n=624$ QDs, 4AP 8h $n=421$ QDs, $p=5.4 \cdot 10^{-7}$. **Syn**: t_0 $n=252$ QDs, 8h $n=173$ QDs,
23 $p=0.2$, 2 cultures. **(H)** Quantification of explored area EA of $\alpha 2$ GABA_AR after 8 h of
24 4-AP application. **Extra**: t_0 $n=1869$ QDs, 8h $n=1092$ QDs, $p=7.8 \cdot 10^{-14}$. **Syn**: t_0 $n=$
25 753 QDs, 8h $n=516$ QDs, $p=0.07$. **(I)** Quantification of $\alpha 2$ GABA_AR diffusion

1 coefficients after 48 h of 4-AP exposure. **Extra:** t0 n= 624 QDs, 4AP 48h n= 631 QDs,
2 p= 0.04. **Syn:** t0 n= 252 QDs, 48h n= 251 QDs, p= 0.8. 2 cultures. **(J)** Quantification
3 of explored area EA of $\alpha 2$ GABA_AR after 48 h of 4-AP application. **Extra:** t0 n= 1092
4 QDs, 48h n= 1890 QDs, p= $1.5 \cdot 10^{-6}$. **Syn;** t0 n= 558 QDs, 48h n= 750 QDs, p= 0.3. **(K)**
5 Quantification of $\alpha 2$ GABA_AR dwell time DT after 8 h or 48 h of 4-AP application.
6 Calculations were done for trapped or passing QDs at inhibitory synapses. **Trapped:**
7 t0: n= 116 QDs, 8 h: n= 84 QDs, 48 h: n= 43 QDs, 0-8h: p= 0.2; 0-48h: p= 0.02;
8 **Passing:** t0: n= 67 QDs, 8 h: n= 46 QDs, 48 h: n= 43 QDs, 0-8h: p= 0.2; 0-48h: p=
9 0.1. In A, C-F, K, data are presented as mean \pm SEM. *P \leq 0.05; ***P \leq 0.001 (Mann
10 Whitney Rank sum test). In G-J, data are presented as median values \pm 25%-75% IQR.
11 *P \leq 0.05; ***P \leq 0.001 (Kolmogorov-Smirnov test). In all graphs except in C, values
12 were normalized to the corresponding control values.

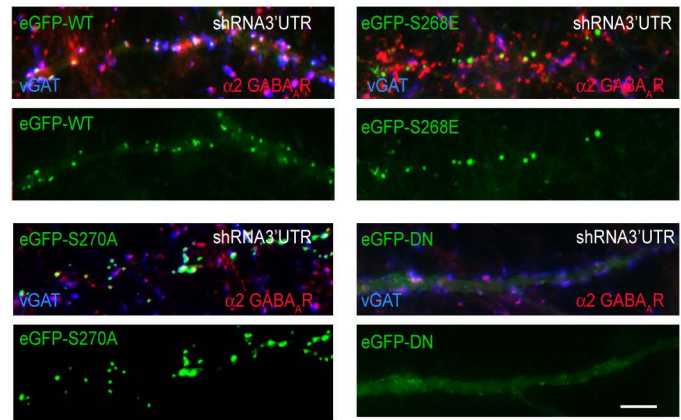
13

14

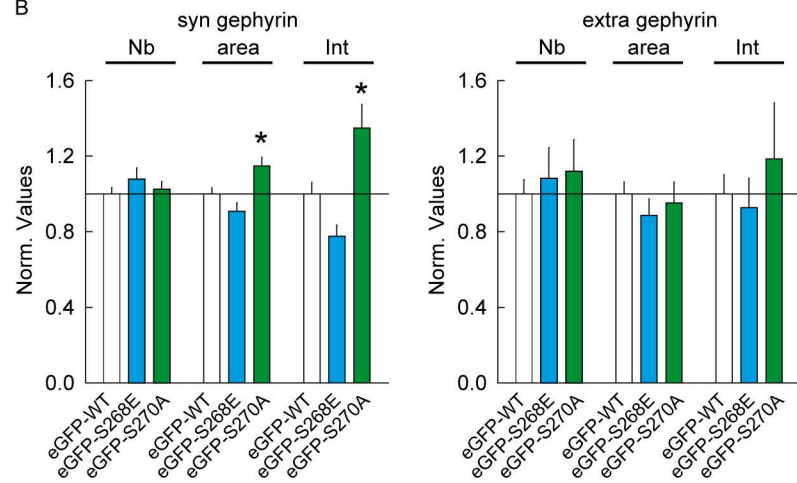
15

Figure 1

A



B



C

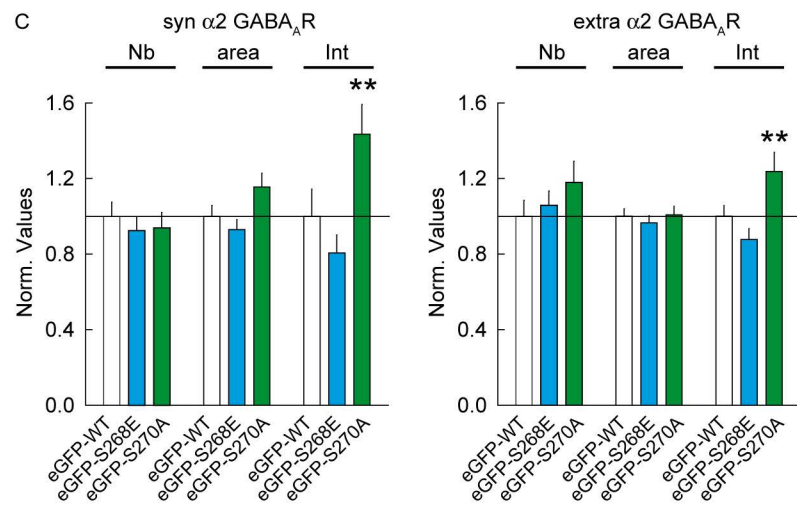
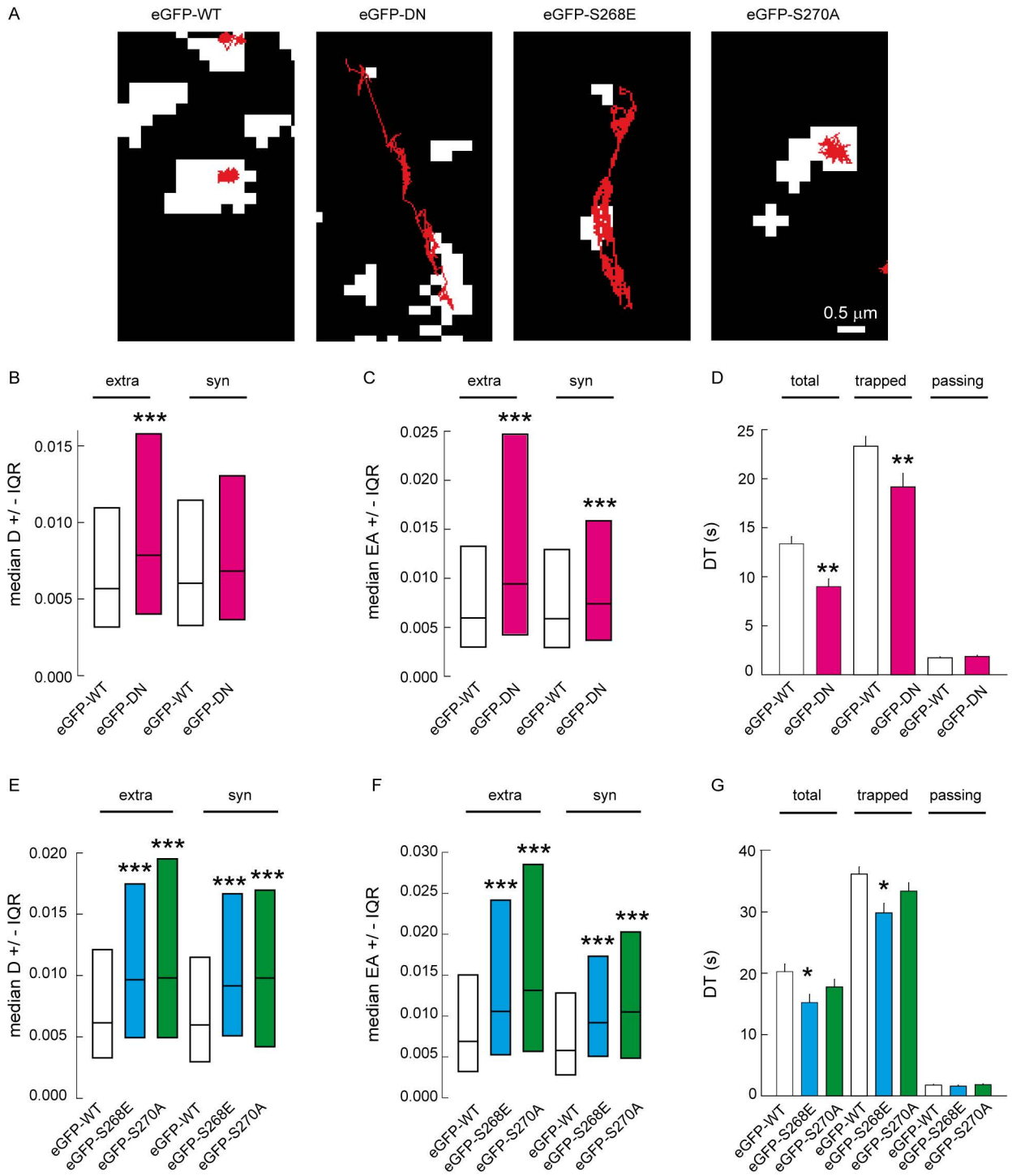
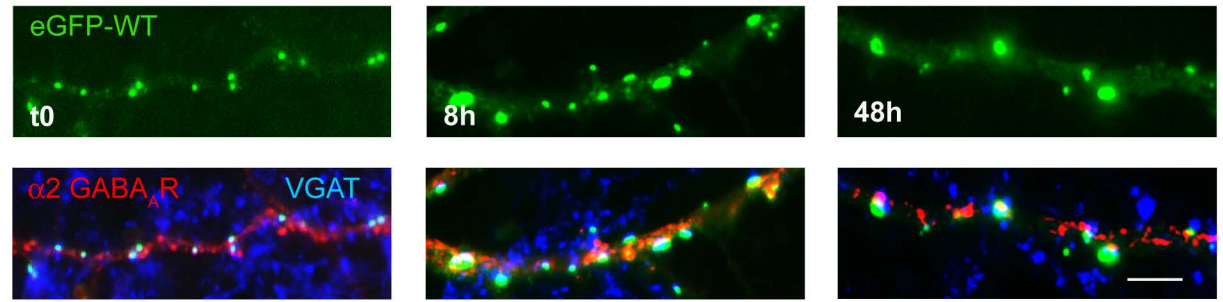


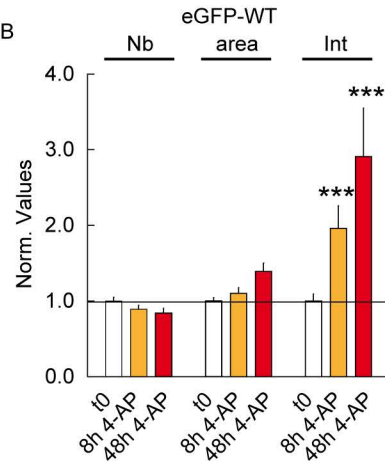
Figure 2



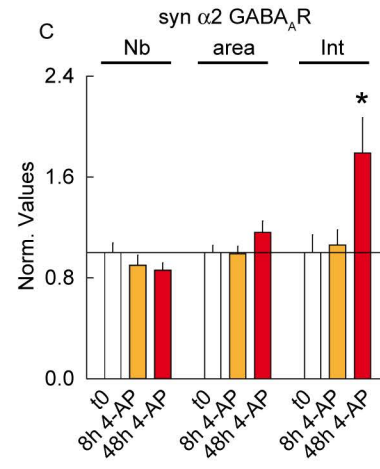
A



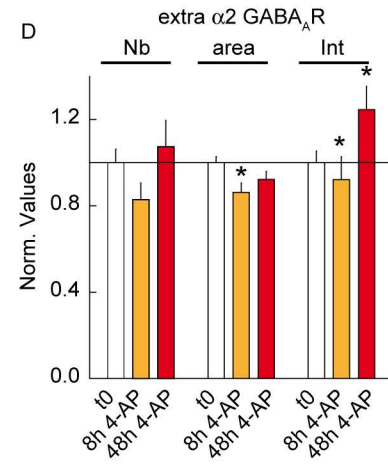
B



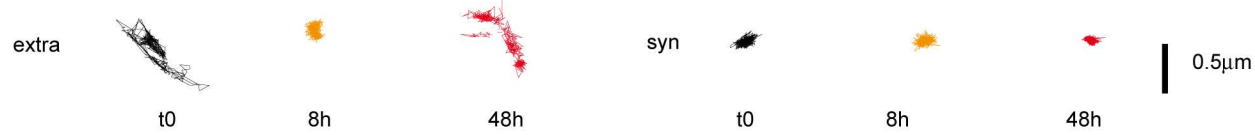
C



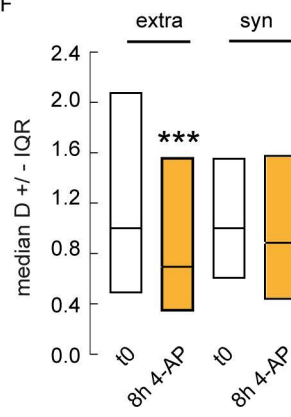
D



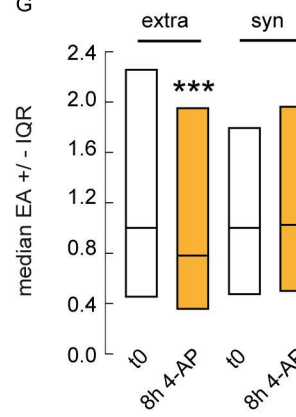
E



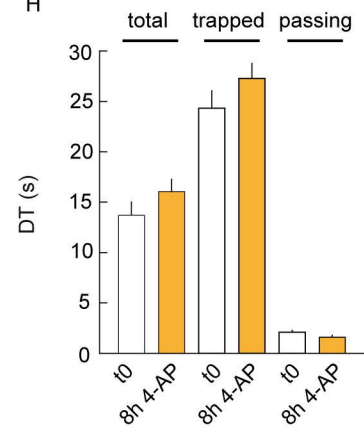
F



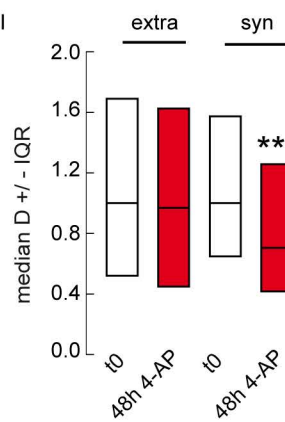
G



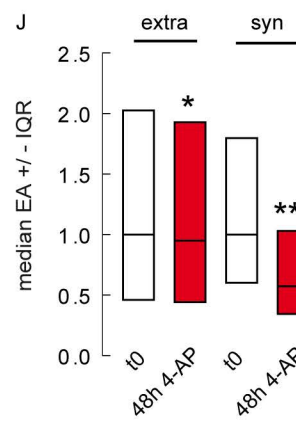
H



I



J



K

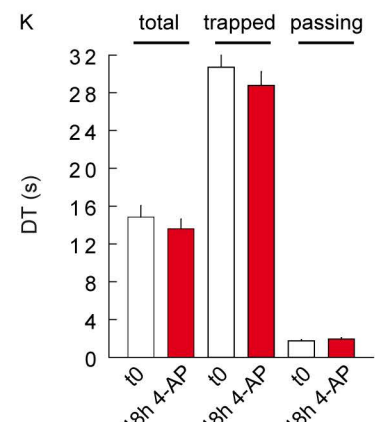
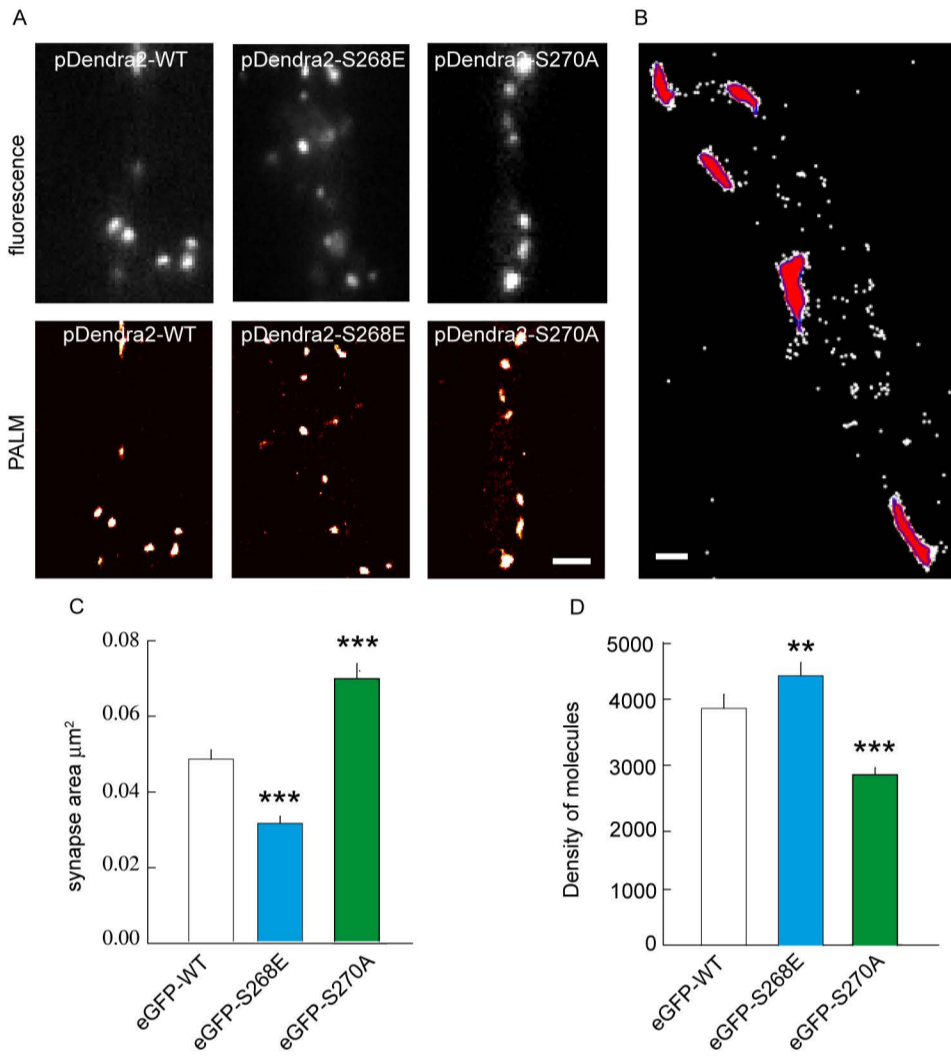
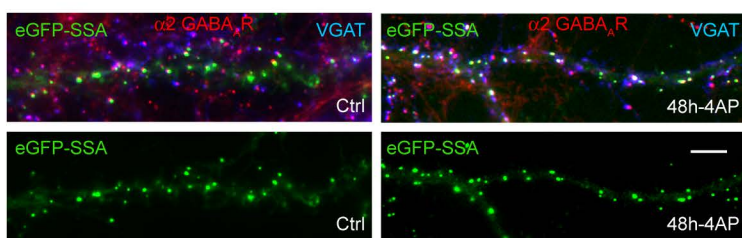


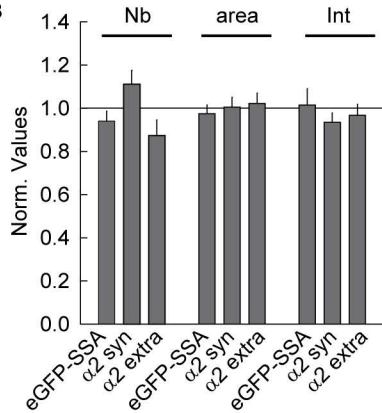
Figure 3



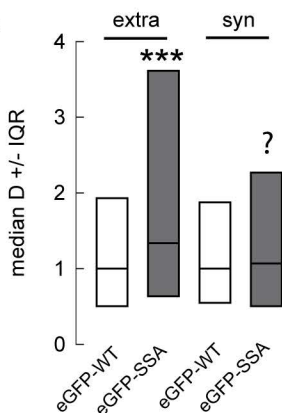
A



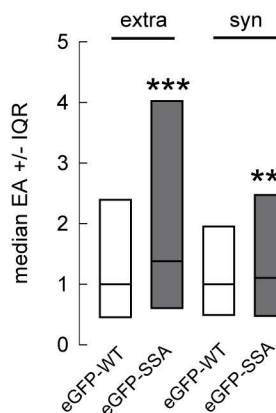
B



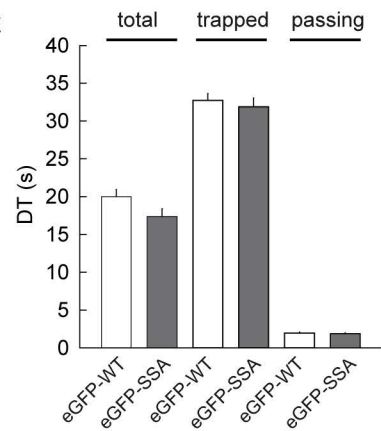
C



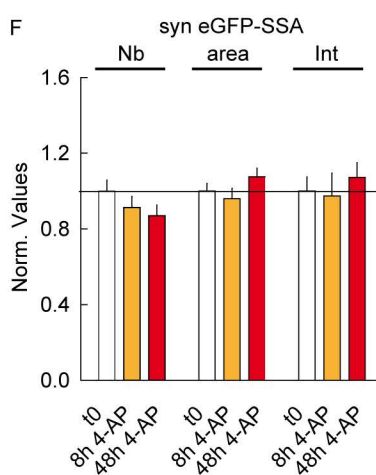
D



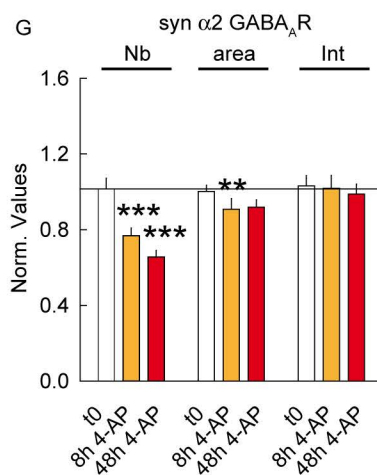
E



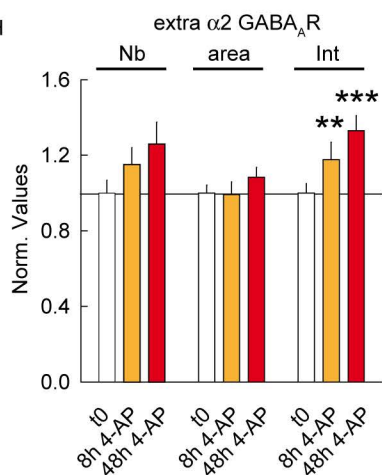
F



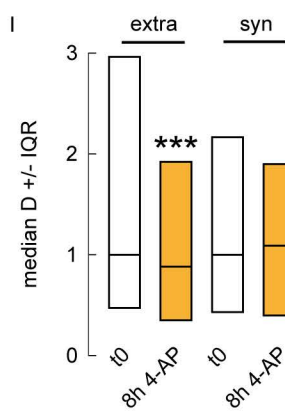
G



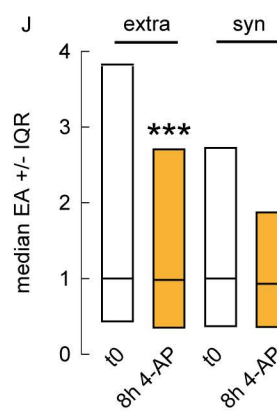
H



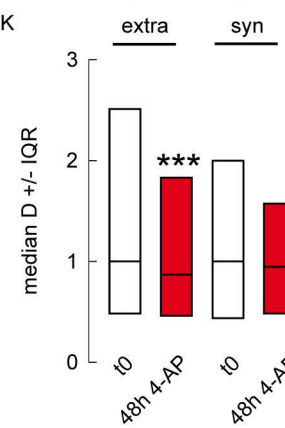
I



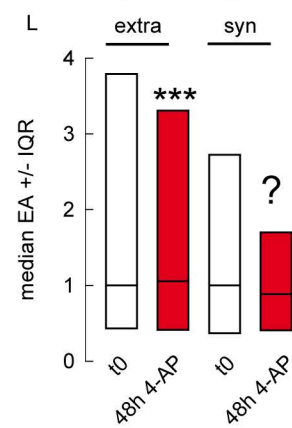
J



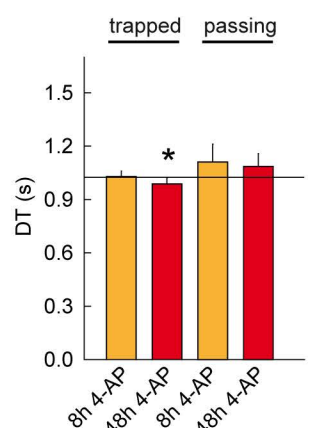
K



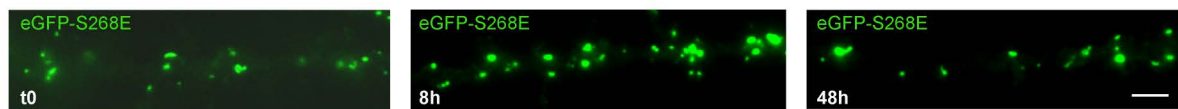
L



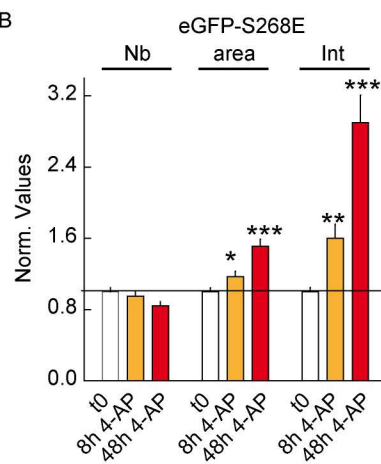
M



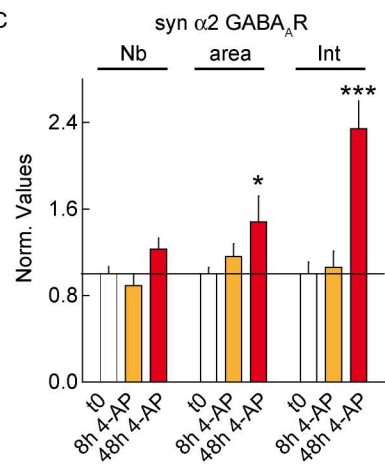
A



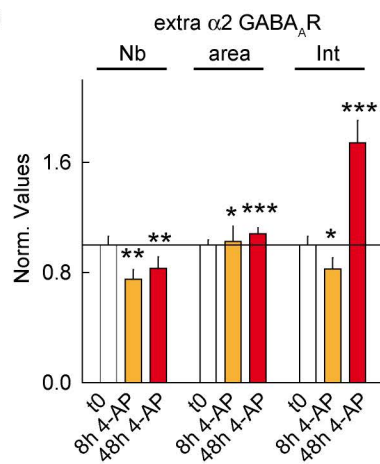
B



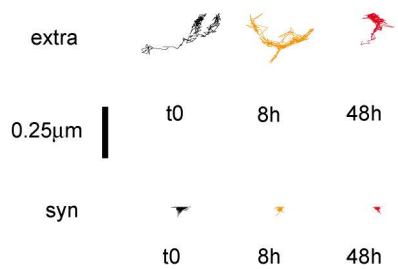
C



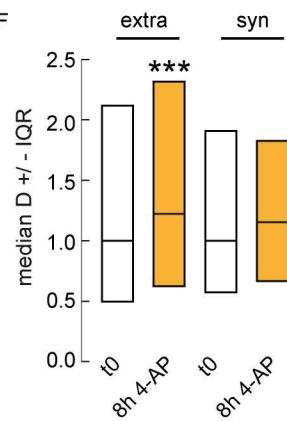
D



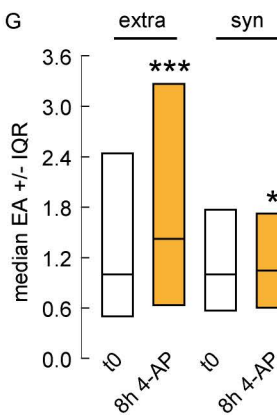
E



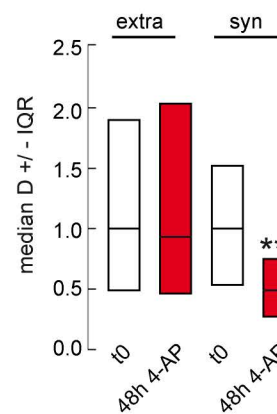
F



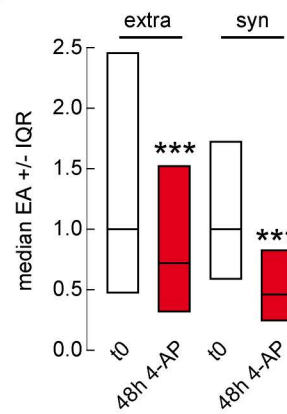
G



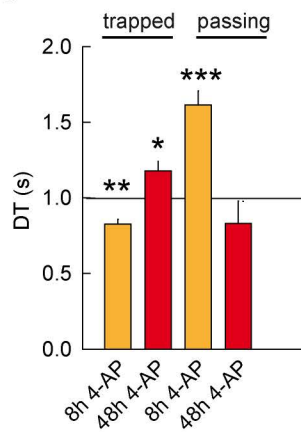
H



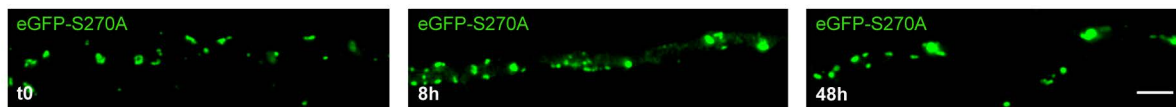
I



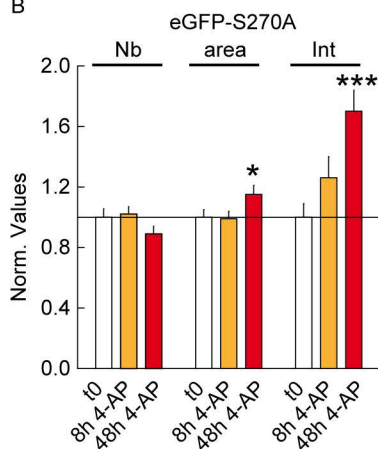
J



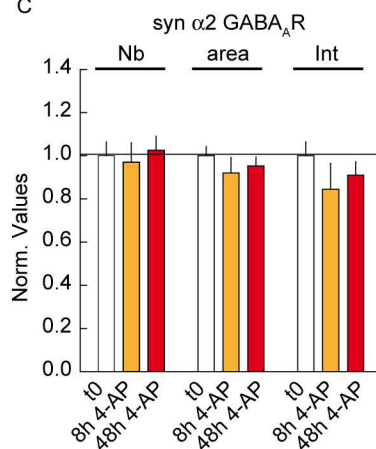
A



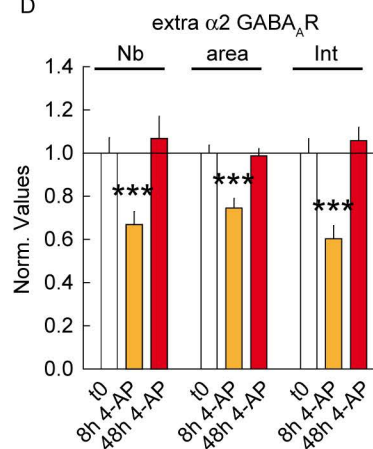
B



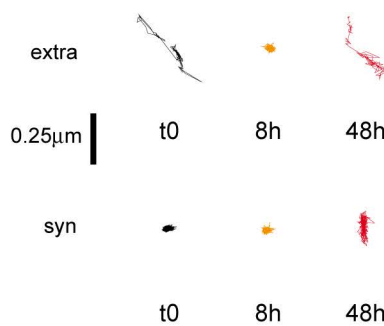
C



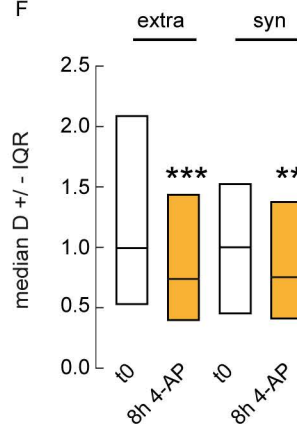
D



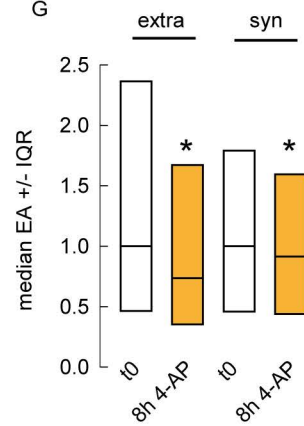
E



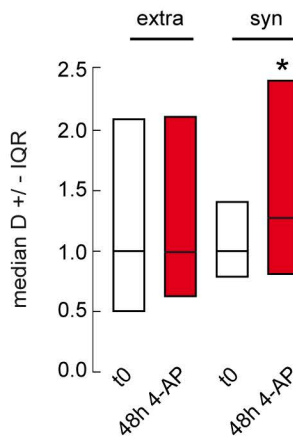
F



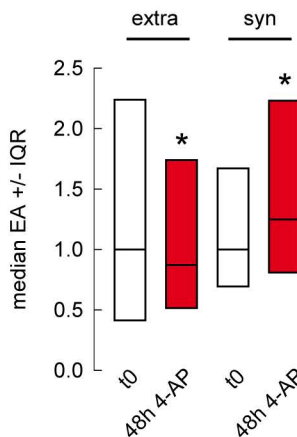
G



H



I



J

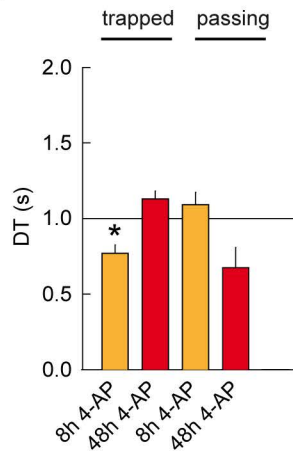


Figure 8

